Review Vol. 10, No. 11 / November 2023 / Optica 1511

Quantum optical memory for entanglement distribution

Yisheng Lei,[1,2,3,†] Faezeh Kimiaee Asadi,[4,†] Tian Zhong,[5] Alex Kuzmich,[6] Christoph Simon,[4] and Mahdi Hosseini[1,2,3,*]

[1]Elmore Family School of Electrical and Computer Engineering, Purdue University, West Lafayette, Indiana 47907, USA
[2]Department of Physics and Astronomy, Purdue University, West Lafayette, Indiana 47907, USA
[3]Department of Electrical and Computer Engineering and Applied Physics Program, Northwestern University, Evanston, Illinois 60208, USA
[4]Institute for Quantum Science and Technology, and Department of Physics & Astronomy, University of Calgary, 2500 University Drive NW, Calgary, Alberta T2N 1N4, Canada
[5]Pritzker School of Molecular Engineering, University of Chicago, Chicago, Illinois 60637, USA
[6]Department of Physics, University of Michigan, Ann Arbor, Michigan 48109, USA
[†]These authors contributed equally to this work.
*mh@northwestern.edu

Received 21 April 2023; revised 29 September 2023; accepted 29 September 2023; published 7 November 2023

Optical photons are powerful carriers of quantum information, which can be delivered in free space by satellites or in fibers on the ground over long distances. Entanglement of quantum states over long distances can empower quantum computing, quantum communications, and quantum sensing. Quantum optical memories are devices designed to store quantum information in the form of stationary excitations, such as atomic coherence, and are capable of coherently mapping these excitations to flying qubits. Quantum memories can effectively store and manipulate quantum states, making them indispensable elements in future long-distance quantum networks. Over the past two decades, quantum optical memories with high fidelities, high efficiencies, long storage times, and promising multiplexing capabilities have been developed, especially at the single-photon level. In this review, we introduce the working principles of commonly used quantum memory protocols and summarize the recent advances in quantum memory demonstrations. We also offer a vision for future quantum optical memory devices that may enable entanglement distribution over long distances.

https://doi.org/10.1364/OPTICA.493732

1. INTRODUCTION

Quantum optical states such as entangled photons can carry quantum information enabling distribution of quantum information in a network setting [1–4]. However, without quantum memories, the fiber-based communication distance is limited to a few hundred kilometers due to losses in fibers, which exponentially degrades the degree of quantum correlations. For this reason, quantum memories were proposed as part of a quantum repeater [5–11] to extend the communication distance. Quantum memories storing entangled photons can themselves be entangled. As seen in Fig. 1, entanglement between neighboring memories can be established by Bell state (or joint) measurement on nearby initially unentangled memories. Subsequent measurement eventually leads to the creation of entanglement between memories in distant nodes. The information can then be teleported from node A to Z without directly sending quantum states, $|\psi\rangle$, through the channel [12,13]. A quantum network of this kind has applications in distributed quantum computing, global parameter estimation using entangled sensors, and secure communication [2,14,15]. Other applications of quantum optical memories include deterministic single photon [16,17] or multi-photon [18,19] generation, coherent optical-to-microwave transduction [20], quantum imaging [21], enhanced quantum sensing [22], non-destructive photon detection [23,24], linear optical quantum computing [25], and fundamental science in space [26].

In this review, we discuss the basic concepts of light storage as applied to atomic quantum memories and review recent advances in quantum memory development.

2. TUTORIAL

A. Basic Concepts

In the simplest form, quantum optical signals can be delayed using delay lines such as a fiber loop or a pair of mirrors increasing the propagation length, L [see Fig. 2(a)]. To implement an atomic quantum memory, on the other hand, quantum fluctuation from an optical field should be coherently mapped to stationary excitations of atomic spins [31,32] [see Fig. 2(b)]. The mapping should be ideally reversible and on-demand, and the process should not add noise to the retrieved optical state. Consider a simple optical qubit in a superposition of two number states $|0\rangle$ and $|1\rangle$ written as $\alpha|0\rangle + \beta e^{i\theta}|1\rangle$. In practice, other types of qubit encodings,

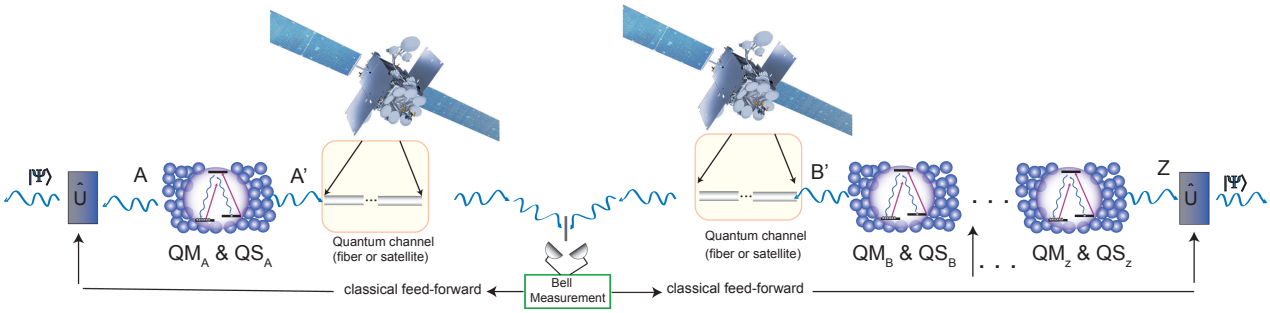

Fig. 1. Illustration of a quantum memory application in optical entanglement distribution. A long communication channel is divided into multiple links with quantum memories (QM) and quantum sources (QS) at their ends. Joint measurement (or Bell state measurement) of photons from neighboring quantum memories projects the state of memories into an entangled state. Repeating the measurement until the first and last memories are entangled by multiple entanglement swapping operations results in entanglement distribution between memories A and Z without a long-distance quantum channel connecting the two nodes. The quantum channels connecting the memories can be fiber or satellite links.

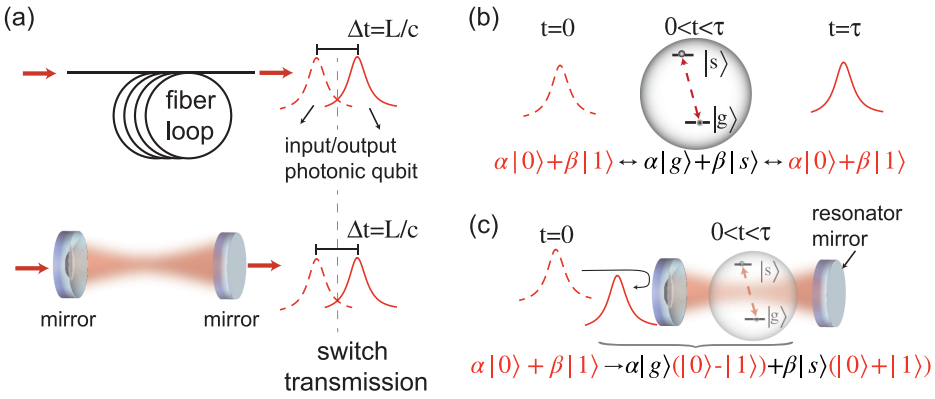

Fig. 2. (a) A fiber loop (top) or a pair of mirrors (bottom) can be used to delay optical qubits by controlling the propagation length L. (b) A single or ensemble of atoms can be controlled to coherently and reversibly map quantum information to/from a photon from/to atomic coherence. (c) An atom inside a low-loss optical resonator can enhance light–atom interactions to the point that reflecting a single photon off the cavity mirror can result in the entanglement between the photon and the atomic spin [27–30].

e.g., time-bin or polarization qubits, are used for long-distance communication. To store information in an atomic memory, the amplitude and phase of the qubit should be transferred to coherence between two energy levels of an atom, e.g., $|g\rangle$ and $|s\rangle$, written as $\alpha|g\rangle + \beta e^{i\theta}|s\rangle$. The process does not necessarily store the energy of the photon but just the information encoded in α/β and θ. In atomic systems, the storage essentially corresponds to a coherent and reversible mapping of flying electromagnetic excitations into stationary qubits.

We first classify quantum optical memories (QOMs) into two categories: linear atomic memories (LAMs) and nonlinear atomic memories (NLAMs).

We draw a distinction between atomic and non-atomic systems. In the former, which is the focus of this review, information is mapped to atomic coherence, while in the latter, optical information is delayed or effectively stored through light propagation in various media such as fiber, free-space, or optical resonators [16,33,34]. Active switching of transmission in these systems can enable controllable retrieval. Other types of non-atomic storage can be achieved using optomechanical systems [35,36] where optical coherence is mapped onto coherent oscillation of a micro or nanomechanical oscillator.

An ensemble of atoms (or atom-like qubits) in free space [37–41], inside low-Q optical resonators [42–47], or near waveguides [48–52] can serve as LAM media. Coherent mapping of quantum information between flying qubits (photons) and stationary qubits (e.g., atoms, ions, superconducting qubits) can occur in the form of exchanging a single collective excitation. In such a case, a collection of atoms shares a single excitation that can be mapped to/from a flying photon. The LAM media operate in the linear regime where different optical or atomic qubits act independently of one another. In this regime, memory properties including the directional probability of photon emission and the amount of photon–photon phase shift are mostly independent of the number of atoms in the memory. A pair of entangled photons stored inside two spatially separate memories can result in the entanglement of the two atomic memories. A typical entangled photon pair generated via a spontaneous process, e.g., spontaneous parametric down-conversion (SPDC) [53] or spontaneous Raman scattering (SRS) [54], can also be stored to create entanglement between quantum memories, albeit non-deterministically. There are various LAM protocols that enable the storage of flying qubits including electromagnetically induced transparency (EIT) [37,55], controlled reversible inhomogeneous broadening (CRIB) [56,57], gradient echo memory (GEM) [58], Raman storage [59–61], and atomic frequency comb (AFC) [62,63], to name a few. As we shall see, the SRS process can also be used for time-delayed photon pair generation where during the delay time, information (half of the entangled state) is stored in atoms that play the roles of both the source and

the memory. This enables the implementation of entanglement between memories [6].

On the other hand, nonlinear memories or NLAMs rely on nonlinear atom–light interactions to create entanglement between photons and atoms [see Fig. 2(c)]. A single atom inside a high-cooperativity optical cavity can nonlinearly interact with a photon such that an electromagnetic field emitted by the atom can interfere with itself modifying the emission rate of the atom inside the cavity. In this scenario, the spontaneous emission into free space can be suppressed, and highly directional emission and efficient interaction can be achieved. As the result, NLAM media can enable deterministic entanglement between photons and atoms. Instead of using the strong atom–photon interactions, NLAM can also be achieved without high-Q optical cavities and using strong atom–atom interaction realized, for example, between two Rydberg atoms [64,65]. In this case, spontaneous emission of high-order photon numbers, which produce noise, are suppressed via the Rydberg blockage effect, making the process of atom–photon entanglement nearly deterministic.

B. Absorptive LAM Protocols

In general, LAMs can be realized through an absorption or emission process. In this section, we review absorptive LAM protocols. Consider a three-level Λ-type atomic system, consisting of one ground state $|1\rangle$, a meta-stable state $|2\rangle$, and an excited state $|3\rangle$. A detuned control field of Rabi frequency Ω_c is applied on the $|2\rangle - |3\rangle$ transition while a quantum field is coupled to the $|1\rangle - |3\rangle$ transition with a coupling strength g, and a detuning Δ, as shown in Fig. 3. The total Hamiltonian of the system is $\hat{H} = \hat{H}_0 + \hat{H}_I$, where $\hat{H}_0$ is the Hamiltonian of the free atom and the quantum field given by

$$\hat{H}_0/\hbar = \sum_{m=1}^{N} \left(\hat{\sigma}_{33}^{(m)} \omega_{13} + \hat{\sigma}_{22}^{(m)} \omega_{23} \right) + \int \hat{a}_k^\dagger(\omega_k) \hat{a}_k(\omega_k) \mathrm{d}k, \quad (1)$$

where the sum is over N atoms with atomic operators for atom m described by $\hat{\sigma}_{ij}^{(m)} = |i\rangle_m\langle j|$. Here, $\hat{a}_k$ is the annihilation operator of the quantized field mode k, and ω_{ij} is the $|i\rangle - |j\rangle$ transition frequency. The term $\hat{H}_I$ also describes the coupling between the fields and atoms. Under the rotating wave approximation (where rapidly oscillating terms are ignored since they eventually average out to zero) and dipole approximation (where the transition matrix elements between states are written in terms of the transition dipole operator $\hat{d}$), this Hamiltonian can be written as [66]

$$\hat{H}_I/\hbar = -\sum_{m=1}^{N} \left(\int g \hat{a}_k e^{-i\omega_k t} \hat{\sigma}_{31}^{(m)} e^{ikz} \mathrm{d}k + \Omega_c \hat{\sigma}_{32}^{(m)} e^{-i\omega_c t + i\phi_c} + \mathrm{H.c.} \right). \quad (2)$$

Here, $g \simeq \langle 3|\hat{d}.\hat{E}_p|1\rangle/\hbar$, $\Omega_c \simeq \langle 3|\hat{d}.E_c|2\rangle/\hbar$, E_c ($\hat{E}_p$) is the control (quantum probe) field vector, c is the speed of light, ω_c ($\omega_p = \omega_k$) is the control (quantum probe) light frequency, and ϕ_c is the relative driving phase of this laser.

Assuming all atoms are equally coupled to the field, we can simplify the integration and describe a monochromatic quantum field with a slowly varying operator $\hat{\mathcal{E}}(z,t) = \int dk \hat{a}_k e^{ikz}$ that interacts with the ensemble with the effective coupling strength $\sqrt{N}g$. Using a Heisenberg equation, $\partial \hat{O}/\partial t = [\hat{O}, \hat{H}]/i\hbar$, we can write the following Maxwell–Bloch equations in a rotating frame [66–68]:

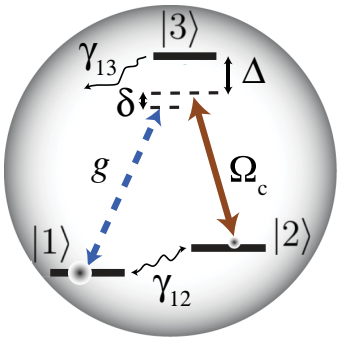

Fig. 3. Energy-level diagram for a Λ-type atom driven by control and probe fields. For simplicity, the detuning is set to be the same for both transitions (i.e., zero two-photon detuning). Δ is one-photon detuning, δ is two-photon detuning, and γ_{ij} is damping rate between levels i and j.

$$\begin{aligned} \partial_t \hat{P} &= -(\gamma_{13} + i\Delta)\hat{P} + i\Omega_c \hat{S} + ig\sqrt{N}\hat{\mathcal{E}}, \\ \partial_t \hat{S} &= -(\gamma_{12} + i\delta)\hat{S} + i\Omega_c^* \hat{P}, \\ (\partial_t + c\partial_z)\hat{\mathcal{E}} &= ig\sqrt{N}\hat{P}. \end{aligned} \quad (3)$$

Here, we defined $\hat{P}(z,t) = \sqrt{N}\hat{\sigma}_{13}(z,t)$ and $\hat{S}(z,t) = \sqrt{N}\hat{\sigma}_{12}(z,t)$ as polarization and spin–wave operators, respectively, where $\hat{\sigma}_{13}(z,t)$ and $\hat{\sigma}_{12}(z,t)$ are the slowly varying collective atomic operators [66], γ_{13} (γ_{12}) is the amplitude damping or decoherence rate of the $|3\rangle \leftrightarrow |1\rangle$ ($|2\rangle \leftrightarrow |1\rangle$) transition (introduced to the Bloch equations to account for damping), δ is the two-photon detuning, and $\Delta = \omega_{13} - \omega_p$ is one-photon detuning as shown in Fig. 3. Below, we ignore the decay channel $|3\rangle \leftrightarrow |2\rangle$, and use $\gamma = \gamma_{13}$ for simplicity.

The above equations of motion can be used to describe various absorptive memories discussed below. For instance, the condition $\Delta = 0$ leads to EIT, and $\Delta \gg \gamma$ describes off-resonant Raman absorption. By tailoring the distribution of atomic frequencies or applying reversible broadening via external fields, one can engineer atom–light detuning Δ to model protocols such as AFC, CRIB, or GEM. In the absence of state preparation, one can further extend the CRIB model to the ROSE (revival of silenced echo) memory protocol. In these protocols, after storage the excitation can be mapped to a long-lived spin state using a control optical π pulse. On atomic resonance, considering a frame moving with the speed of light, the steady-state solution to the above equations enables us to derive the optical density, $d = g^2 NL/(\gamma c)$, where L is the medium length, as a measure of absorption or interaction strength. Single-photon absorption maps optical coherence to atomic polarization P. To implement certain protocols specially in solids, the absorption process and transfer to spin state S are separated in time using optical π pulses. The transfer to spin state can be done directly via a two-photon transition, particularly when hot or cold atomic gas is used. In the off-resonant Raman scenario (i.e., $\Delta \gg \gamma$), the steady-state solution can be used to define an effective Raman coupling rate given by $g' = g\sqrt{N}\Omega_c/\Delta$, which determines the off-resonance interaction strength mapping the electric field directly to the atomic spin, $\hat{S}$.

In general, it is beneficial to place the atomic system inside a cavity to realize efficient light–matter interactions. When a cavity has low loss and a small interaction volume (i.e., in the high-cooperativity regime), the spontaneous emission and coupling rates can also be modified. Absorptive memories with near-unity efficiency can be implemented when low-Q cavities are employed [68–70]. In the above system, if we assume the $|1\rangle - |3\rangle$ transition of atoms is coupled to a quantized cavity radiation mode, the Heisenberg equation of motion for the slowly varying cavity mode annihilation operator can be written as

$$\dot{\hat{\mathcal{E}}} = ig\sqrt{N}\hat{P} - \kappa\hat{\mathcal{E}} + \sqrt{2\kappa}\hat{\mathcal{E}}_{in}, \tag{4}$$

where 2κ is the cavity decay rate, and $\hat{\mathcal{E}}_{in}$ is the cavity input field. In the resonant condition, combining Eqs. (3) and (4) enables us to define cooperativity written as $C = g^2/(\kappa\gamma)$ (for $N = 1$), which is a unitless parameter used to measure the cavity-enhanced interaction strength. Collective cooperativity can also be defined as NC. When $C \ll 1$, the cavity interaction can still enhance the efficiency of the memory to store and retrieve optical information. When $C \gtrsim 1$, the so-called strong coupling regime is reached enabling near-deterministic atom–light entanglement, as will be discussed in Section 2.D. In the following, we review some of the widely used absorptive memory protocols used to realize LAM.

1. Electromagnetically Induced Transparency

EIT memory uses a relatively intense control laser to reversibly imprint a state of light (i.e., probe field) onto an atomic state [37,71]. When the fields are in a two-photon resonance condition, a transparency window in the absorption spectrum of an otherwise opaque atomic system will be induced at the frequency of the probe laser. As soon as the probe is spatially compressed inside the medium (since its group velocity is greatly reduced), its coherence can be adiabatically transferred from the atomic polarization mode to the spin mode by progressively reducing the control field power to zero (i.e., bringing the probe field to a complete halt) [38]. To retrieve the stored photon, one needs to gradually turn on the control field. The group velocity of light inside the medium is proportional to the control laser power and inversely proportional to the optical density, d. In contrast, the EIT bandwidth or width of the transparency window is (inversely) proportional to (control power) $\sqrt{d}$. Thus the delay-bandwidth produces scales with $\sqrt{d}$. At high optical densities, however, one needs to be careful to reduce the four-wave mixing (FWM) noise [72].

2. Autler–Townes Splitting

Similar to the EIT, the ATS is an optically controlled memory [73]. However, the mapping process of the latter has a non-adiabatic (i.e., fast) nature as we turn off the control field abruptly. Here the probe field is absorbed through the ATS peaks [74], generated by the ac-Stark splitting, and its coherence is mapped into the spin mode through a non-adiabatic exchange process mediated by the atomic polarization, $\langle\hat{P}\rangle$, described in Eq. (3). As a non-adiabatic memory protocol, ATS is more flexible in terms of the required control field power and optical depth compared to the adiabatic protocols [75]. In principle, the smaller the optical depth and control field power, the less four-wave mixing noise. However, in turn, ATS is only efficient for the storage of input fields whose bandwidths (at full-width half-maximum) are larger than the linewidth of the transition in resonance with the probe field (i.e., referred to as broadband regime).

3. Off-Resonant Raman

The detuned version of the EIT memory when both control and probe fields are detuned from the excited level, as shown in Fig. 3, is called off-resonant Raman memory [59,76,77]. This scheme is also established based on the adiabatic elimination of the polarization mode. However, here, the Raman scattering causes the storage of the probe field. Compared to the EIT, the detuned nature of the Raman makes it less susceptible to fluorescence noise and enables large-bandwidth storage possible. These benefits, however, come at the expense of a stronger control field to compensate for the weak coupling caused by the off-resonant operation [66,73,78]. As a result, the four-wave mixing noise is typically higher in Raman memory than in EIT quantum memory. An effective way to suppress the FWM noise is to use a cavity in resonance with the probe field but antiresonance with the noise field [79].

4. Controlled Reversible Inhomogeneous Broadening

In principle, depending on the retrieval direction and shape of the inhomogeneous profile, the inhomogeneous broadening (i.e., distribution of atomic frequencies) can decrease the memory efficiency by reducing the effective optical depth (or cooperativity in cavity-coupled memories) [80]. On the other hand, CRIB is an engineered absorption-based quantum memory that benefits from an artificially produced inhomogeneous broadening [56,57]. Realization of this protocol in solids requires the generation of a narrow spectrally isolated absorption line (i.e., spectral tailoring) from an inhomogeneously broadened line. This can be done via the optical pumping of the rest of the population into an auxiliary energy level. An external magnetic or electric field gradient is then used to broaden the absorption line controllably and reversibly. This tailors the single-photon absorption spectrum, and the stored excitation can then be mapped to S after absorption to extend the storage time. Broadening can be accomplished with an electric field gradient and the linear Stark effect in rare-earth-doped solids with a permanent dipole moment [81]. This results in the absorption of the probe field by the broadened line. Following the absorption, the external field is turned off, allowing the population to be transferred to a ground state using an optical pulse. Re-emission of the stored photon can occur later by transferring the population back to the excited state and reversing the sign of the external field to create a photon echo. When the propagation direction of the probe is parallel to the direction of the external field variation, the resulting scheme is called gradient echo memory (GEM) [58] or longitudinal variant of CRIB that enables on-demand retrieval. The GEM protocol can be very efficient [82,83] as it suppresses re-absorption, and it allows for arbitrary and coherent control of optical information [84–86].

In contrast to EIT or Raman memories whose multimode capacity scales as $\sqrt{d}$, CRIB is a memory protocol with a multimode capacity that scales linearly with the optical depth [87].

5. Atomic Frequency Comb

AFC is another engineered absorption-based scheme that has attracted considerable attention [62]. Unlike the CRIB protocol, which only needs a single narrow absorption line, AFC requires

many periodic absorption lines (a comb), in which each pair of nearest-neighbor peaks is separated by a frequency δ_{AFC}. Such a comb can be prepared by optical pumping techniques to selectively transfer atoms into a meta-stable state (i.e., tailoring the absorption profile). Here, the bandwidth of the photon to be stored is limited from below (above) by peak spacing (comb overall width). In this memory protocol, after a specific time determined by $1/\delta_{\mathrm{AFC}}$, the rephasing of atomic excitations results in the automatic re-emission of the photon. To address the limitation of pre-determined re-emission, optical control fields can be employed to temporarily map the coherence of the stored optical excitation (P) to a long-lived ground state as a spin-excitation mode (S), after absorption. This also results in longer storage times. Alternatively, combining CRIB and AFC protocols for each absorption line can also make the retrieval on-demand [88]. Another approach is to use a dc-Stark shift to create a π phase difference in the atomic ensemble, and later apply another electric field to rephase the system to retrieve the photon [47,89,90].

It has been shown that, unlike many other memory protocols, the multimode capacity of the AFC is not limited by the optical depth [87]. To be more precise, the ratio of the excited state storage time to the duration of the stored pulse determines how many temporal modes can be stored in an AFC quantum memory. This ratio is independent of the optical depth, making AFC a promising candidate for designing multimode memories.

6. Other Protocols

Besides the commonly used protocols listed above, there are more memory schemes. The traditional two-pulse photon echo techniques suffer from spontaneous emission and gain due to population inversion onto excited states. Four-level photon echo schemes [91] are proposed to mitigate the issues by using more energy levels and spectral filtering, but imperfect π pulses still leave some atoms in the excited states, which makes them difficult to implement at the single-photon level. The revival of silenced echo (ROSE) is another technique [92] in which spatial phase mismatch is created between an input pulse and first rephasing π pulse to suppress the first echo. Sending another π pulse then rephases the atomic ensemble. This method also suffers from imperfect π pulses. A photo-echo memory has also been proposed by combining four-level photon echo and ROSE [93]. Stark echo modulation memory (SEMM) [94,95] has also been introduced by utilizing inversion symmetry of the linear Stark effect in solids, which can create a π phase difference among two types of frequency shifts in the atomic ensemble, instead of using spatial phase mismatching. Four-wave mixing in the atomic ensemble can also be used for delaying or storing quantum light [96]. Two-photon off-resonant cascaded absorption (ORCA) has been used to demonstrate intrinsically noise-free quantum memory [97,98]. Recently, fast ladder memory (FLAME) was demonstrated to store light in electronic orbitals of rubidium vapor, with limited storage time due to the finite lifetime of the excited state [99,100]. Using off-resonant Faraday interactions in warm vapor cells, ms-long quantum storage has been demonstrated [40,101]. It was also shown that coherence can be mapped to noble-gas spin via spin–exchange collisions to reach hour-long coherence in hot atomic vapor [102–104].

C. Emissive LAM Protocols

In emissive memories, the excitation is heralded by the emission of an idler photon controlled by an external laser pulse. The spontaneous emission of the idler photon detected in a certain detection mode gives rise to the creation of stored atomic excitation that is entangled with the idler photon. Subsequent retrieval of the atomic excitation can be obtained by reversing the process using a strong laser thus creating a signal photon entangled with the idler.

When a spontaneously scattered photon is emitted into the detection mode, the ensemble N of atoms initially in the ground state, $|G\rangle = |g_1 g_2 \ldots g_N\rangle$, is transferred to a collective excitation $|S\rangle = \frac{1}{\sqrt{N}} \sum_i |S_i\rangle$, where $|S_i\rangle = |g_1 g_2 .. s_i .. g_N\rangle$ is the atomic state when atom i is excited to the meta-stable state $|s_i\rangle$. The summation over i denotes the sum of all permutations. The state of the system can then be written as an entangled state $|\psi\rangle = a|G, 0\rangle + b|S, 1\rangle$, where 0 and 1 denote zero and one photon states, and a and b are the normalization coefficients. A similar process can be used to generate polarization photonic qubits as shown in Fig. 4(a).

Using the above-mentioned process, the DLCZ scheme [6] was first proposed as a means for long-distance quantum communication. In this scheme, an optical laser field is used to establish a Raman transition between the two ground states of a Λ-type atomic ensemble. This results in a collective excitation mode within the ensemble. Later, a second laser can be used to retrieve the stored collective excitation as a propagating field. Idler photons from two distant ensembles can then be directed to a 50:50 beam splitter (BS) to perform join measurement. The latter erases the which-path information of photons. The detection of a single photon after BS results in the generation of entanglement between the ensembles [109] [see Fig. 4(a)]. The recalled photons from two neighboring ensembles can then be directed to another BS. A successful Bell state measurement results in entanglement swapping between the two pairs of entangled ensembles, by which entanglements can be extended to long distances.

In 2003, several groups proposed a two-photon interference scheme that can also be used to generate entanglement between remote qubits [110–112]. In this scheme, qubits are initially prepared in the excited state, which can later decay into either of the ground states. As a result, an entangled state between the emitted photon and the qubit can be created. Two emitted photons, each coming from a qubit, meet at a BS located in between qubits for a Bell state measurement. The detection of two photons by two different detectors projects the joint state of distant qubits into a Bell state.

A single-photon interference scheme can also be implemented to achieve an "event-ready" Bell test [110]. Moreover, a double-heralded single-photon interference scheme can also generate entanglement between distant qubits [113]. Using this scheme, the first loophole-free Bell test has been demonstrated [114].

D. Nonlinear Atomic Memories

The LAM protocols discussed so far rely on absorptive or emissive processes integrated with spontaneous photon generation to create probabilistic photon–atom or atom–atom entanglement. The strength of light–atom interaction can be quantified with cooperativity as defined earlier for an atom inside a cavity. In free space, the cooperativity can also be defined [115] for a single atom as $C_{fs} = 6/(kw)^2$, where k is the wavenumber and w is the waist of the light field at the location of the atom. The free-space and cavity

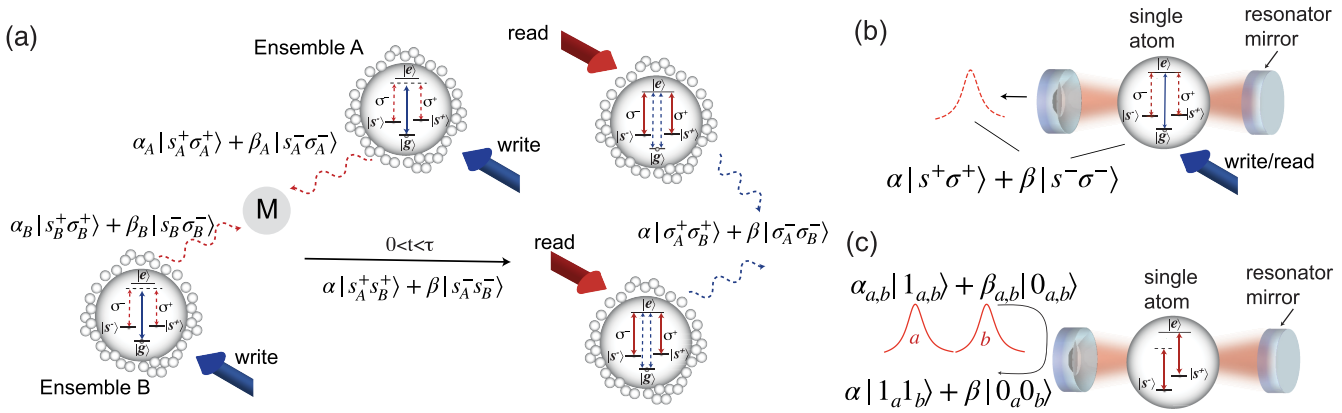

Fig. 4. (a) An ensemble of atoms can generate polarization qubits via a spontaneous Raman scattering process while entangled with a single collective spin excitation stored in the ensemble. Joint measurement (M) of two photonic qubits (red) generated from distant ensembles via two "write" laser fields can project the two ensembles into an entangled state [105]. Collective excitations of the two ensembles can be mapped to flying entangled qubits (blue) after a desired storage time. (b) The probability of atom–photon entanglement in (a) can be enhanced using high-cooperativity interaction of a single atom inside an optical resonator. (c) Another scheme for photon–atom and photon–photon entanglement is shown where the reflection of the first photonic qubit off a high-cooperativity cavity containing a single atom can create near-deterministic atom–photon entanglement [30,106]. Subsequent reflection of a second photonic qubit b and detection of the atomic state can create near-deterministic photon–photon entanglement [107,108].

cooperativities are ideally related by a factor that is proportional to the finnese of the cavity. For N atoms in free space, the collective cooperativity is written as NC_{fs}. At the resonant condition, the collective cooperativity and the optical density are related by the following relation: $d = 2NC_{fs}$, which quantifies the collective interaction strength. Two absorptive QMs require high optical densities for efficient storage of an entangled photon pair. This, however, does not imply that the two memories can be entangled deterministically. The entanglement probability is bounded by the probability of photon pair generation, which for spontaneous sources are about a few percent. As we discussed above, emissive QMs can be used to directly generate atom–photon entanglement. When $C_{fs} \ll 1$, uniform scattering in all directions leads to probabilistic atom–photon entanglement. This picture is still valid for N randomly distributed atoms, where scattering intensity in any given direction scales linearly with N. We note that for ordered atomic ensembles and in the superradiance regime, the interaction can be nonlinear leading to directional photon scattering scaling with N^2. Other ways to reach the nonlinear regime of atom–photon interaction include using high-Q cavities or dipole–dipole interactions. In this section, we discuss the principles of NLAM in the context of strong light–atom interactions inside high-Q cavities and strong atom–atom interactions based on Rydberg atoms, as methods for near-deterministic generation of entanglement.

1. Strong Cavity Interaction

Photon–atom interactions can be enhanced by optical resonators to overcome the probabilistic limitation in LAMs. Such interaction is key to deterministic entanglement creation between atomic and photonic qubits, as well as superconducting qubits, and are used in various quantum technologies. We note that simply placing an atom inside an optical cavity does not make its interaction with a photon less probabilistic. Certain interaction parameters need to be engineered to reach the strong coupling regime. We refer to this interaction regime as the high-cooperativity regime, where an atom or a photon state can interfere with itself. If losses are small and interactions can happen faster than the decay rate of the atom (cooperativity $C > 1$), the EM field of the photon can interfere with the atom and suppress or enhance the emission. The interaction is therefore nonlinear at the single-particle level.

On the atomic and cavity resonance, the ratio of the scattered power, $P_{4\pi}$, and the transmitted power, P_{tr} to the incident power, P_{in}, can be expressed in terms of the cooperativity [115] as $P_{4\pi}/P_{in} = 2C/(1+C)^2$, and $P_{tr}/P_{in} = 1/(1+C)^2$.

It can be seen that at high cooperativities, the transmission and scattering are suppressed to the point where the photon is reflected from the cavity with high probability, given by $C^2/(1+C)^2$. This, however, does not indicate that the photon will not enter the cavity or not interact with the atom. It is the interaction with the atom that gives rise to such "cavity blocking." Cooperativity is also a measure of scattered power into the cavity mode relative to the 4π solid angle. For this reason, a photonic qubit reflected off a high-cooperativity cavity can be entangled with the intra-cavity atom with near-unity probability. The strong interaction in this form can be used to create near-deterministic atom–photon or photon–photon entanglement. As seen in the example in Fig. 4(b), directional Raman scattering of an optical polarization qubit $\alpha|\sigma^+\rangle + \beta|\sigma^-\rangle$ can be entangled with the atomic spin states, $|s^+\rangle$ and $|s^-\rangle$ [116]. In the reflection scenario [example shown in Fig. 4(c)], the state $\alpha_{a,b}|1_{a,b}\rangle + \beta_{a,b}|0_{a,b}\rangle$ refers to a photonic qubit a or b, in superposion of time bins (or other bases) represented by $|1\rangle$ and $|0\rangle$. An incident photonic time-bin qubit is only reflected when an intra-cavity atom is in a certain ground state with maximum interactions. As the result, after reflection of the first photonic qubit a, the atom and photon are in an entangled state $|\psi\rangle = |1_a, s^+\rangle + |0_a, s^-\rangle$. Reflection of the second photonic qubit b followed by detection of the atomic state can map the state of the two photonic qubits into an entangled state $\alpha|1_a 1_b\rangle + \beta|0_a 0_b\rangle$. The strong (weak) interaction of a photon with an atom in $s^+(s^-)$ results in a differential phase shift that when combined with measurement on the atomic qubit entanglement can be achieved [107]. Such entanglement can be ideally deterministic in the low-loss and high-cooperativity regimes.

2. Strong Atom–Atom Rydberg Interaction

Rydberg-level interactions in an atomic ensemble can be used to generate single-photon pulses in a near-deterministic fashion. When the ensemble is resonantly driven on the ground to a Rydberg transition, strong interactions between Rydberg atoms produce level shifts that suppress state components containing more than one excitation [117,118].

Bariani *et al.* have proposed a spin–wave dephasing mechanism that achieves the same goal of preparing a singly collective state of no more than one excitation [119]. The dephasing approach has been used to describe a number of experiments aimed at quantum light generation in Rydberg ensembles [64,65,120–122]. In this approach, a short excitation pulse creates a collective state of multiple excitations. Following the excitation, the state components containing more than one excitation undergo dephasing as a result of the distribution of the interaction shifts between pairs of atoms. Only the singly excited component is then available for a phase-matched emission process. The maximum population of a singly excited collective state produced via the dephasing mechanism is limited to $1/e$ [119], while the Rydberg excitation blockade, in principle, allows for unity efficiency [123].

If only part of the collective atomic excitation is mapped into a retrieved field, an entangled state is created between the atomic excitation and a propagating light field [64,65]. Separating the generation of single photons and their storage will allow to both achieve single-photon generation and memory-light mapping efficiencies in excess of 80% [123,124] and memory storage times in excess of 1 s [125].

E. Multiplexed Quantum Memories

Consider a small linear system of memories and sources as shown in Fig. 5 where photon–memory entanglement can occur with probability p. The success probability of entanglement creation between two adjacent memories separated by distance L_0 after Bell state measurement (BSM) is given by $P_0 = p\eta_t\eta_d$, where η_t and η_d are the efficiencies of channel transmission and detection, respectively. The transmission efficiency of the fiber link is $\eta_t = e^{-L_0/2L_{att}}$, where $L_{att} = 22$ km (assuming 0.2 dB/km fiber loss). Detection efficiency is bounded by BSM probability, i.e., η_d. For spontaneous sources, $p \sim 0.05$ is limited by the probability of having higher-order photon numbers. η_m is the memory efficiency. In a multilayer network and for n levels of entanglement swapping (nesting layers) in a repeater network by using a single-photon scheme, the entanglement rate [7] can be expressed as

$$R_e = \frac{c}{L_0}\frac{\eta_t\eta_d^{n+3}\eta_m^{n+2}p}{3^{n+1}\prod_{k=1}^{n}[2^k-(2^k-1)\eta_m\eta_d)]}. \quad (5)$$

As an example, for eight memories ($n = 2$, four elementary links) extending the communication distance to $L = 2^2L_0 = 1000$ km, assuming both memory and detection efficiencies to be 0.9, one entanglement event can be achieved around every 1 h! Although this entanglement rate is much faster compared with direct fiber links (less than one event every 10^{10} s), in this traditional approach, due to the low entanglement rate and need for quantum memories with hour coherence times, such a network has limited practical use.

To go beyond such traditional communication schemes, provided the technology is available, one can simultaneously process multiple modes of photons using multimode BSMs, multimode sources, and memories [7,126]. The photon generation probability can, in principle, approach unity where strong light–atom interactions [64] are employed. Considering strong cavity interactions, the probability of generating photon–atom entanglement can increase by more than an order of magnitude. Moreover, assuming m (spatial, temporal, or spectral) modes processed in parallel, the communication rate can linearly increase with m.

Instead of parallel processing of multiple modes m, multiplexed processing [127] of entanglement can be implemented to enhance the communication rate. Multiplexed quantum optical processing refers to the ability to perform Bell state measurement (BSM) on the multiple numbers of modes shared between two nodes. The results are then fed forward to perform subsequent measurements at the next layer, only between the entangled modes established at the first layer. Therefore, multiplexing relies on switching under feed-forward control, a crucial functionality that benefits from the co-existence of classical signals in the channel. In the limit of low memory lifetimes, the communication rate scales as $(mP_0)^{2^n}$ for $mP_0 \ll 1$, while it is $mP_0^{2^n}$ for parallel processing (n is the number of nested layers in the network). The rate scaling is also significant in the intermediate memory lifetimes (a few 100 ms) resulting in practically useful communication rates. According to Ref. [127], in the high-memory-lifetime limit, the multiplexing only marginally improves the rates when compared to parallel schemes.

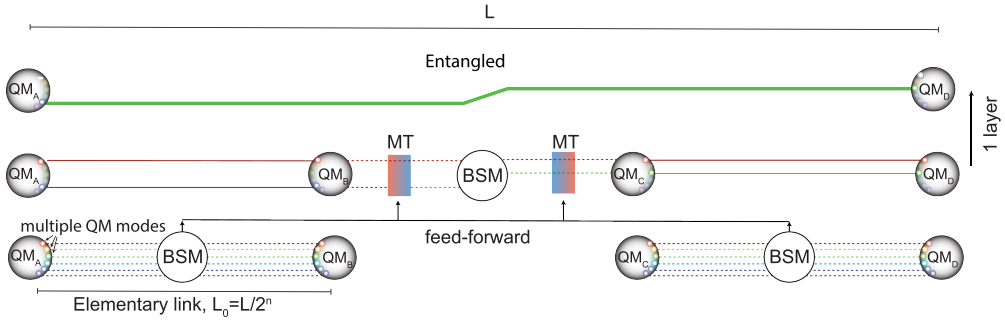

Fig. 5. Example of a linear network consisting of quantum memories (QM) and Bell state measurement (BSM) stations. Entanglement creations at elementary links and one layer of entanglement swappings (nested layer $n = 1$) are used to create end-to-end entanglement between memories separated by distance L. Quantum memories are considered to support multiple atom–photon entanglement modes (temporal, spectral, or spatial) shown by different colors. Results of BSM at the elementary links can be fed forward to the next layer to perform mode transformation (MT) on remaining entangled photons followed by BSM on corresponding modes.

F. Quantum Memory Properties

The performance of quantum memories can be assessed by different figures of merit discussed below. The **fidelity** of memory shows how close the retrieved quantum state is to the input quantum state by quantifying the overlap between them. In general, infidelity can happen due to different mechanisms such as loss, four-wave mixing noise, decoherence through interactions, and thermal effects.

In some memory protocols where we aim for single-photon storage, the completion of the scheme is conditioned on the retrieval of a specific outcome (e.g., the re-emission of a single photon). One can then define a conditional fidelity, which quantifies the overlap of the emitted single-photon state with the input single-photon state. Another quantity that is sometimes used to quantify memory noise is μ_1, defined as the input mean photon number needed to produce a unity signal-to-noise ratio at the output [128].

Memory **efficiency** quantifies the energy of the output compared to the input, or more specifically, the success probability of recovering a photon. The efficiency can be reduced by different types of loss present in any system (e.g., absorption, scattering). In ensemble-based systems, the collective interference effect boosts efficiency. On the other hand, in single atomic systems, using cavities can enhance light–matter interaction and therefore efficiency. For certain protocols, the re-absorption of the re-emitted light can limit the maximum efficiency to below 54% [62]. In backward retrieval or using impedance-matched cavities, however, efficiency can be near-unity. Although the efficiency of the memory process itself (internal efficiency) can be high, the end-to-end efficiency may be small due to the low fiber coupling efficiency or losses due to filters or other optical elements.

In addition to communication times as an important factor influencing achievable repetition rates of repeater protocols, the **bandwidth** of a quantum memory also determines the achievable communication rate through the multimode capability and repetition rates. In principle, the longer the duration of a pulse, the smaller the achievable bandwidth. The maximum attainable bandwidth depends on the memory protocol and characteristics of the storage system.

Storage time is another important key factor of memory that can be limited by a medium's coherence time. In particular, in long-distance quantum communication applications, the memory storage time should be at least comparable with the entanglement generation time, e.g., the time required to establish entanglement between two distant nodes in addition to the time it takes for a classical signal to go back over the same distance and notify us about the outcome of measurements. To increase the storage time in atomic systems, one can use zero-first-order Zeeman transitions that have zero gradient with respect to the magnetic field and are therefore less sensitive to the field fluctuations [129]. Additionally, in most atomic systems, lowering the temperature can slow down decoherence processes and therefore extend the storage time. Dynamical decoupling techniques such as Carr–Purcell–Meiboom–Gill (CPMG) sequences [130,131] can also suppress noise effects in a given system [132,133].

The selection of the **wavelength** is mainly influenced by the memory application and memory medium. For example, telecom wavelengths are recommended for communication through optical fibers as they have minimal absorption during transmission [134]. On the other hand, for free-space communications, diffraction is the main source of transmission loss [135].

In general, the wavelength of the recalled photon can be changed using nonlinear interactions or transduction mechanisms [136–139]. By using difference-frequency or sum-frequency generation processes, the wavelength can be converted to the telecom wavelength for long-distance propagation in fibers [140–143]. It is also possible to utilize cold atoms for wavelength conversion [144,145]. Telecom quantum memory with hot Rb vapor has also been demonstrated by cascaded two-photon absorption [98]. Furthermore, to avoid limitations in memory platform selection, photon pair sources can be used to separate entanglement generation and storage processes [7,146,147].

Multimode capacity is the capacity to store independent quantum states simultaneously in a single memory. Multiplexing is especially important for improving communication rates over long distances [7,127]. Multiple degrees of freedom can be employed in a multimode memory, including temporal, spectral, spatial, and angular. To further expand the mode's capacity, some of these degrees of freedom can also be combined [148]. Spatial multiplexing can be achieved in cold-atom systems by segmenting a dense ensemble of cold atoms [149,150] and temporal multiplexing by storing multiple temporally distinct modes [151] as high as memory's delay-bandwidth product. Wave-vector multiplexing is another approach for multimode storage in a single atomic cloud with feed-forward control feasibility [152,153]. Orbital angular momentum and vortex beams of light can also be used for multiplexing [154,155]. Among solid-state quantum memory systems, rare-earth-ion-doped crystals are also uniquely identified with their multimode quantum storage capability using different degrees of freedom [156–158]. In particular, the relatively large inhomogeneously broadened absorption profile of these ions has made temporal multiplexing a convenient approach. In this regard, the storage of more than a thousand temporal modes using rare-earth ions has set a new record in temporal multiplexing [159]. Multiplexed storage of spatial, temporal, and spectral modes in a rare-earth crystal has also been demonstrated for close to 2000 modes and a projected mode capacity of more than 1.5×10^5 [148,160]. The feed-forward control of spectral modes has also been shown in rare-earth crystals [161].

3. STATE OF THE ART

The efficient and deterministic distribution of quantum entanglement is key to developing future quantum networks [2]. To date, several entanglement-distribution demonstrations have been carried out with and without memories. Early entanglement distributions were demonstrated more than a decade ago [109,162–164]. Most advanced demonstrations of entanglement distribution to date include: three-node quantum entanglement distribution using cold atomic memories with overall efficiency 10^{-8} [165], memory-less ground–space integrated quantum key distribution (QKD) network over 4600 km [166], memory-based QKD with rate enhancement relying on asynchronous BSMs [106], eight-node all-optical quantum communication with probabilistic bi-party entanglement distribution [167,168], entanglement of solid-state QOMs [147,169,170], faithful quantum state transfer between a cold atomic ensemble and a rare-earth-doped crystal [171], and quantum teleportation through a middle node by using built-in nuclear spin quantum memory in a nitrogen-vacancy (NV) center in diamond [172].

Below we discuss the most advanced QOMs and their application in the context of quantum communication networks. Table 1

Table 1. Summary of Most Recent Advances in Stand-Alone LAM (Absorptive and Emissive QM) Developments in Different Platforms Highlighting Measured Fidelity ($\mathcal{F}$) or Autocorrelation ($g^{(2)}$), Internal Efficiency (η_{in}) or End-to-End Efficiency (η_{e2e}), Storage Time (τ_s), Bandwidth ($\Delta\omega$), Operating Temperature (T), Applied Magnetic Field (B), Wavelength (λ), State Being Stored (SP, Single Photon; SPCS, Single-Photon-Level Coherent State; CS, Coherent State), and Multimode Capacity (MC)[A]

	Diamond Defects	RE Crystal (Er^{3+})	RE Crystal (Pr^{3+})	RE Crystal (Eu^{3+})	Laser-Cooled Atoms	Hot Vapor
$\mathcal{F}$ or $g^{(2)}$	0.89[a], 0.94[b]	0.97[c]	0.98[e], 0.95[f]	0.85[g]	> 0.99[h], 0.92[j]	0.97[k], **0.18**[l], **0.02**[m]
η_{in} or η_{e2e}	NR	0.01[c], 0.22[d]	0.69[e], 0.62[f]	0.07[g]	0.68[h], 0.85[i], ~0.26[j]	0.78[k], **0.01**[l], **0.24**[m]
τ_s	13 ms[a], 75s[b]	5 ns[c], 660 ns[d]	1.3 μs[e], 2 μs[f]	20 ms[g]	1.2 μs[h], 15 μs[i], 100 ms[j]	100 ns[k], 160 ns[l], 12 ns[m]
$\Delta\omega$ (MHz)	NR	8k[c], 6[d]	0.14[e], ~1[f]	3[g]	~1[h,i]	< 1[k], 370[l]
T (K)	0.1[a], 3.7[b]	1[c], 1.5[d]	3[e], 3.2[f]	3.5[g]	20 μ[h,i], 90 μ[j]	368[k], 322[l], 338[m]
B (T)	0.3[a], 0.04[b]	0.06[c], 7[d]	0[e,f]	1.35m[g]	0[h,i,j]	0[k,l,m]
λ (nm)	737[a], 637[b]	1532[c], 1536[d]	606[e,f]	580[g]	852[h,i], 795[j]	795[k,l], 780[m]
State	SPCS[a,b]	SP[c], SPCS[d]	CS[e], SPCS[f]	SPCS[g]	SPCS[h], SP[i], SPCS[j]	SPCS[k], SP[l,m]
MC	NR	1650[n]	10^5 (est.)[o]	> 100[p]	225[q]	60[r]

[A]Memories based on rare-earth-ion-doped solids in Refs. [*c*, *d*, *f*, *n*, *p*] demonstrate a fixed delay and not on-demand storage. Corresponding references and their assigned memory categories are *a*: emissive QM [173], *b*: emissive QM [174], *c*: absorptive QM [175], *d*: absorptive QM [176], *e*: absorptive QM [82], *f*: absorptive QM [177], *g*: absorptive QM [178], *h*: absorptive QM [179], *i*: absorptive QM [180], *j*: emisive QM [181], *k*: absorptive QM [44], *l*: absorptive QM [182], *m*: absorptive QM [183], *n*: absorptive QM [160], *o*: absorptive QM [148], *p*: absorptive QM [184], *q*: emissive QM [150], and *r*: emissive QM [19]. Promising results were also obtained with other rare-earth ions such as Nd^{3+} [169], Tm^{3+} [185], and Yb^{3+} [186] (not listed in this table). Semi-classical storage in Eu^{3+}-doped crystal with 1 h coherence time has also been shown [187].

Table 2. Summary of Recent Demonstrations of Entanglement Distribution Using Atomic Memories Highlighting Measured Fidelity ($\mathcal{F}$) or Concurrence ($\mathcal{C}$), Link Distance (d), Entangled-Pair Probability (p), Entanglement Rate (R_e), and Wavelength (λ)[A]

	Quantum Dots	Diamond Defect	RE Crystals	Trapped Ions	Laser-Cooled Atoms	Hot Vapor
$\mathcal{F}$ or $\mathcal{C}$	0.55[a], 0.6[b]	0.54[c]	0.92[d], 0.8[e]	0.58(0.88)[f], 0.86[g]	0.72(**0.38**)[h], 0.62[i]	**~0.004**[j]
d (m)	5[a], 2[b]	30(2)[c]	50[d], 10[e]	520[f], 50k[g]	22k(50k)[h], 33k[i]	0.3[j]
p (%)	~7[a], ~7[b]	5[c]	~0.007[e]	~70[f], 50[g]	3.8(1.5)[h], ~1[i]	~0.04[j]
R_e (Hz)	2.3k[a], 7.3k[b]	**~0.01**[c]	1.4k[d], **~0.3 m**[e]	**~0.5(~ 0.06)**[f], >1(est.)[g]	**~7 m**(~ 1.54)[h], **~0.01**[i]	<1(est.)[j]
λ (nm)	953[a], 968[b]	637[c]	606 & 1436[d], 880[e]	854[f], 854 & 1550[g]	795 & 1342[h], 780 & 1517[i]	850[j]

[A]Corresponding references as *a*: [188], *b*: [189], *c*: [170], *d*: [147] (light–matter entanglement with RE crystal over a metropolitan network of field-deployed fibers has been reported in a recent paper [190].), *e*: [169], *f*: [191], *g*: [192], *h*: [105], *i*: [193], and *j*: [194]. Estimated values (est.) are authors' estimations based on reported quantities in corresponding references. Entanglement rates (R_e) shown in bold were achieved for two-photon or three-photon interference.

summarizes the most recent significant advances in the development of stand-alone QOMs in different platforms, which include experiments performed in a semi-classical or quantum regime. We highlight recent demonstrations of low-noise storage that excel in efficiency, storage time, or bandwidth. It is important to note that nearly all memories developed to date do not achieve the highest performance in all metrics. For instance, certain demonstrations achieve high bandwidth at the expense of efficiency, while others exhibit long storage time but with lower bandwidth and efficiency. We also summarize recent entanglement distribution demonstrations using LAMs and NLAMs between separate nodes in Table 2.

A. Advances in Absorptive Quantum Memories

Many platforms are being used to develop absorptive LAMs, including rare-earth-ion-doped crystals [82,147,159,169,187,195], cold atomic systems [73,124,125,196,197], and hot vapors [19,198–201]. Below, we summarize the most notable results.

Following the first demonstration of an EIT memory in a cold atomic cloud [38], several experiments were carried out to improve light storage using this protocol. In particular, [196] a conditional fidelity beyond 99% (with an efficiency of 85%) has been achieved using rubidium (Rb) atoms [124]. A similar experiment with cold Cs atoms was also reported [180]. Nanofiber-guided memory with a cold atomic ensemble has been demonstrated [48,49].

Using off-resonant Raman memory, an efficiency of up to 82% with an unconditional fidelity of 98% and a bandwidth in the range of 10^2 MHz has also been reported in Rb vapor [61].

Four-wave mixing noise is an important source of infidelity in Raman memories (especially those operating at room temperature) that can be suppressed by engineering interference [202], using cavities to suppress the noise [59,79], or exploiting selection rules [182].

With respect to the multimode capacity, an angularly multiplexed holographic memory based on the Raman protocol has been demonstrated using 60 spin–wave modes in warm Rb vapors [19].

Similar to the Raman scheme, ATS offers storage of broadband input fields. In particular, optimal ATS memory in the broadband regime requires an optical depth that is nearly six times smaller than the one required for an optimal EIT scheme [203]. Using the

ATS memory, a bandwidth of 14.7 MHz [73] and an efficiency of up to 30% [203] have been demonstrated in cold Rb atoms and Bose–Einstein condensate (BEC) platforms, respectively. Recently, theoretical research on cavity-enhanced ATS quantum memory using T centers has also yielded promising results [204].

For a two-level gradient echo memory, low noise storage of optical pulses with an efficiency of 69% has also been obtained in praseodymium (Pr^{3+})-doped crystal [82]. However, the storage time in this experiment was only a few microseconds. Later, using a three-level Λ structured warm rubidium vapor, the recall efficiency of the GEM protocol improved to 87%, but the storage time remained in the same regime [83]. In addition, using the same platform, a recall fidelity of up to 98% has been demonstrated for coherent pulses with around one photon [205]. The same efficiency for storage (i.e., 87%) has also been reported in an ensemble of laser-cooled Rb atoms with storage times of up to 0.6 ms, albeit with a low bandwidth of 210 kHz [206].

Temporal multimode storage using the CRIB has also been studied. It has been shown that to achieve an efficiency of 90% using 100 temporal modes, an optical depth of around 3000 is required [87,126]. Although it is an improvement compared to multimode memories based on EIT and Raman, the required value of optical depth is still unrealistic.

Using AFC memory, a storage bandwidth of 5 GHz has been reported in a thulium-doped lithium niobate waveguide [195]. In Ref. [207], nearly unit conditional fidelity (99.9%) was demonstrated using an Nd^{3+}-doped crystal. Besides, using the linear Stark effect, an extension of the AFC protocol (i.e., Stark-modulated atomic frequency comb) with a recall efficiency of 38% and a short storage time of 0.8 μs has been realized for weak coherent states with a signal-to-noise ratio of 570 [89]. Later, using the same approach, a conditional storage fidelity of 99.3% has been demonstrated [90]. However, in this experiment, the storage time was limited to 2 μs mainly due to the electrically induced broadening of the absorption peaks. In a more recent experiment, using the dynamical decoupling technique and ZEFOZ transitions of Eu^{3+}-doped crystal, the same group reported a storage time of 1 h and a fidelity of 96.4% for coherent laser pulses [187]. Spin–wave storage has been demonstrated in Eu^{3+} [128,178] and Pr^{3+} [146,148,208], and more recently optical spin–wave storage in Kramers ion ytterbium (Yb^{3+}) [186]. Non-Kramers ions such as Pr^{3+} and Eu^{3+} doped in crystals have been used to demonstrate long-time and high-efficiency quantum storage due to their long lifetimes and coherence times, since their electronic spins can be quenched by crystal fields, while Kramers ions such as Er^{3+} and Yb^{3+} suffer from short lifetimes and coherence times due to spin flips and cross-relaxation. Strong magnetic field (>1 T) and low temperature (∼1 K) can greatly increase the excited state coherence time of Er^{3+} doped into yttrium orthosilicate to be 1 ms [209]. In similar conditions, a hyperfine state with coherence time over 1 s has been reported in Ref. [210]. Efficient state preparations have also been developed by the same group, which has achieved 22% storage efficiency after 660 ns for weak coherent pulses [176]. More effective optical pumping methods need to be investigated to prepare atomic frequency combs with better structures and completely empty the hyperfine levels for spin–wave storage.

Cavity-assisted AFC memory allows for highly efficient storage of quantum states. Several experiments using the impedance-matched cavity approach [69,70] have demonstrated cavity-enhanced AFC memory with efficiencies of up to 62% in rare-earth-ion-doped solids [177,211].

The inhomogeneously broadened absorption profile of rare-earth ions doped into solids has been utilized to demonstrate storage of 100 temporal modes in Nd-doped crystal [158]. A more recent experiment used Yb^{3+} doped into a crystal for multiplexed storage of 1250 temporal modes with a bandwidth approaching 100 MHz [159]. Although temporal multiplexing is well suited for the AFC memory [62], spectral and spatial multiplexing can also be performed using this protocol. The storage of a polarization qubit using two spatially separated ensembles of Pr^{3+} doped into a crystal has been demonstrated [157]. In addition, multiplexed storage of weak coherent states into up to 26 spectral modes has been reported in a Tm^{3+}-doped waveguide [161]. More recently, simultaneous storage of 15 frequency bins of a photon pair, where each spectral bin contains nine temporal modes, in a Pr^{3+}-doped waveguide has been demonstrated [156].

Quantum memories storing true single photons generated by quantum dots, or SPDC or FWM processes have been demonstrated and characterized in various types of atomic systems [100,124,158,182,185,197,212]. In rare-earth ions, entanglement generation between remote AFC-based memories has also been reported [147,169]. In the former paper, a multimode AFC memory with 62 temporal modes has been used.

B. Advances in Emissive Quantum Memories

DLCZ-type memories can be used to generate a collective spin excitation in an ensemble of atoms and then recall it on demand as a propagating photon. A DLCZ-based quantum memory with telecom-wavelength conversion and a storage time of 100 ms has been reported in cold Rb atoms [213]. In addition, by confining the same platform inside a ring cavity, to enhance atom–light coupling, a DLCZ memory with a recall efficiency of 76% and a sub-second lifetime has been demonstrated [214]. More recently, 38% memory efficiency (intrinsic retrieval efficiency) and 0.92 fidelity for 0.1 s storage has been achieved [181]. Atomic arrays coupled with nanofiber have been used to generate single collective excitation [50].

Entanglement generations between remote emissive LAMs have been demonstrated using different platforms, such as NV centers [215], hot vapors [194], trapped neutral atoms [216], trapped ions [191,217], atomic ensembles [218], and quantum dots [188,189]. In particular, entanglement has been established among three distant quantum memories, each of which is made up of a laser-cooled Rb atomic ensemble [165]. Later, the same group reported entanglement generation between two laser-cooled atomic memories separated by 22 km (field-deployed fibers) and 50 km (coiled fibers) using a two-photon [110] and a single-photon interference scheme [6], respectively [105]. Entanglement of two single trapped atoms over 33-km telecom fiber has been achieved [193]. More recently, entanglement distribution over 50-km-long fiber spools has been demonstrated using trapped ions [219]. In this experiment, ion–photon entanglement is first generated via a cavity-mediated Raman transition [220]. The generated photons in a middle station are then sent over 25 km of fiber in opposite directions. A deterministic Bell state measurement between nearby ions then projects the state of the remote photons into an entangled state. A multi-node quantum network has been realized with NV centers in diamond [170].

There have been more recent proposals for designing quantum repeaters based on emissive memories [134,221]. Multiplexed memories can help with the entanglement generation rate of a repeater protocol [7,222]. Notably, spatial multiplexing of laser-cooled atomic memories has been achieved that enabled the creation of up to 225 independent memory cells [149,150,197]. Besides, although DLCZ-type memories are not ideal for temporal multiplexing, by combining this memory protocol with an AFC-based rephasing mechanism, a multimode memory with 12 and 11 temporal modes has been demonstrated in an ensemble of $Eu^{3+}:YSO$ and $Pr^{3+}:YSO$, respectively [223,224]. More recently, a multiplexed DLCZ memory with up to 10 temporal modes has been demonstrated in cold Rb atoms [151]. In this experiment, significant noise suppression has been achieved by using a CRIB-based rephasing mechanism and embedding the storage medium in a cavity.

Long-distance entanglement generated between emissive memories has been used to conduct a loophole-free Bell test [114,225].

C. Advances in Nonlinear Atomic Memories

Strong photon–atom interaction inside high-cooperativity cavities can lead to near-deterministic photon–atom entanglement generation [27]. In 2007, a reversible state transfer between light and a single atom trapped in a Fabry–Perot cavity was realized [226]. Later, with a memory efficiency of 9.3%, Raman storage of laser pulses using single Rb atoms trapped inside a single-sided cavity was demonstrated [227]. The same group has also demonstrated the storage of single photons in single atoms [164]. Also, Schrödinger-cat states of entangled atom–light have been deterministically created by cold atoms placed in an optical cavity [228]. Relying on cooperative and directional scattering, the generation of strong photon–photon correlation has also been demonstrated in these systems [229].

In solid-state platforms, a quantum dot inside a nano-beam cavity was used to demonstrate near-deterministic photon–photon entanglement [108], and asynchronous BSMs of two photons have been demonstrated with a SiV center coupled to nanophotonic resonators [106]. Single rare-earth ions have been integrated with nanophotonic resonators for single-shot readout and single-qubit control [230–232].

Moreover, as discussed in the context of Rydberg atoms, a collective Dicke state prepared in an atomic ensemble by the combined action of the excitation blockade and interaction-induced dephasing can be efficiently mapped into a propagating single-photon wave-packet [120]. If only part of the collective atomic excitation is mapped into a retrieved field, an entangled state is created between the atomic excitation and a propagating light field [64,65,233]. An ensemble of atoms can also be used as a source of single photons. By storing a part of the single-photon wave-packet in a separate atomic ensemble containing several million atoms, atom–light entanglement can be achieved. Separating the generation of single photons and their storage will allow to both achieve single-photon generation and memory-light mapping efficiencies in excess of 80% [123,124] and memory storage times in excess of 10 s [125].

D. Advances in QM Materials

Considering materials used for QM implementation, significant advancements are being made in the development of laser-cooled atoms and ions, capitalizing on their long coherence times and multiplexing properties. Moreover, QM systems based on atomic vapor are also under active development, owing to their relaxed experimental requirements. Another promising QM platform is solid-state materials, which hold great potential for on-chip integration.

Using cold atoms, long-life quantum storage (up to a record 16 s) [125], multiplexed quantum storage [150], and memory enhanced entanglement distribution [234] have been demonstrated. More than 1 h of coherence time has been achieved in trapped ions [235]. Storage time of 10 s has been demonstrated in a dual-species trapped-ion system, in which the $^{88}Sr^{+}$ ion acts as a communication qubit and the $^{43}Ca^{+}$ ion serves as a memory qubit [236].

Hot alkali vapors have been used to demonstrate storage time of milliseconds, with anti-relaxation coating on the walls of the vapor cells [17,182,237]. Spin–exchange interactions between nuclear spins of noble gas and hot atomic vapor can be exploited to reach hour-long coherence time [102–104]. Moreover, optical control of nuclear spins of helium-3 gas by metastability exchange collisions has been proposed, which may achieve day-long coherence time [238].

Defect centers and rare-earth ions in crystalline hosts are being considered as suitable platforms for integrated quantum photonic applications. For example, silicon vacancy in 1D photonic crystals was recently used as memory qubits to improve the quantum key distribution rate [106] and rare-earth ions in yttrium orthosilicate and orthovanadate crystals were used for quantum storage [45,90], quantum transduction [239], and spin–photon interfaces [230,231]. The main limitations of the solid-state approach are inhomogeneity in atom/defect properties (such as transition frequency, dipole orientation, location, etc.) and decoherence due to noisy host materials especially when it comes to photonic integration where the emitters are proximal to etched surfaces. A couple of defect systems have emerged in the past years that demonstrate superior properties in both of these regards. Divacancy-defects in SiC can operate as a high-quality spin–photon interface [240] with spin coherence times reaching 5 s [241]. Recently, T-centers in silicon showed significant promise with narrow optical linewidths in the telecom O-band and long-lived spins with millisecond coherence times [204,242]. Some of the rare-earth ions being considered include erbium (Er^{3+}) and ytterbium (Yb^{3+}) ions in a host crystal with telecom or near-telecom transitions and the ability of microwave-optical transduction, respectively [138]. Some of the host materials considered include yttrium orthosilicate (Y_2SiO_5), which has been proven to provide long nuclear coherence times, and lithium niobate on insulator (LNOI), which has multifunctional capabilities. More recently, $CaWO_4$ [243,244] has attracted attention due to its low nuclear-spin-induced decoherence. Y_2O_3 [245–247] is another promising host showing both narrow optical linewidths and millisecond-long spin coherence times. Following the general scalings of spin qubit defect coherence [248], at least a few dozens of known host crystals can provide a magnetically quiet matrix that supports $>$ ms coherence time for spin defects. Many of those are potentially excellent host materials for rare-earth ions, and preliminary optical spectroscopy on a subset of them with favorable point group symmetries has been reported [249,250].

4. VISION

Quantum memories have experienced rapid and broad advances over the last two decades. Still, much room for further developments remains. It is too early at this point to predict the physical platform that will offer the best performance for quantum memories. Given a wide array of material systems under consideration and an equally wide spectrum of EM fields to which these memories can be coupled, there may ultimately not be a single winner, but rather a range of quantum memories that are optimal for particular applications. Below we sketch some of the interesting quantum memory implementations and indicate both the promise and the challenges inherent to them.

Quantum memories based on hot atomic vapors are appealing for deployment in the field due to their less stringent environmental requirements [251], and their scalability using microfabrication techniques [252]. While such quantum memories are often noisy at high optical densities, the noise can be suppressed by employing an optical cavity, or by exploiting selection rules or ladder schemes, which also enable single-photon storage [97,182,183]. Nuclear spins of the noble gas can reach hours-long coherence times [102–104]. While direct optical access in noble gases is often difficult, a binary mixture of alkali and noble-gas atoms can function as a quantum memory with both convenient and strong coupling to light and exceptionally long storage times, and is therefore attractive for quantum repeater implementations [253].

Laser-cooled atomic systems offer excellent storage times, high efficiency and fidelity, and versatile control options. With expected further advances in photonic integration and on-chip atomic traps [254–256], these systems might present sufficiently robust performance in compact packages to be considered for field implementations.

Solid-state systems such as diamond color centers, quantum dots, defects in SiC, rare-earth ions, etc., offer outstanding large-scale integration possibilities. In particular, rare-earth-doped crystals possess seconds- to hours-long coherence times [129,210], with the ability to store telecom-band photons. Large spectral bandwidths and availability of temporal multiplexing protocols are noteworthy strengths of these systems. The electronic spins of the nitrogen-vacancy centers in diamonds have been shown to have millisecond-scale coherence times even at room temperatures, while even longer, second-scale, coherence times are achievable for their nuclear spins [257]. Access to the latter requires mapping quantum states between the electron and nuclear spins. The possibility of designing a quantum repeater using room-temperature NV centers has been discussed in Ref. [258].

Taking advantage of atom–atom or atom–photon interactions under conditions of high cooperativity is promising for achieving near-deterministic approaches for scalable entanglement distribution with quantum memories. Cavity-enhanced interaction of photons with single trapped atoms, ions, or solid-state quantum centers enables deterministic photon–atom entanglement generation [28,106,181,191]. Similar functionalities are offered by ensembles of atoms with strong Rydberg interactions [64]. Extending these approaches to the generation of photonic tree cluster states might make it possible to achieve one-way quantum repeater implementation for entanglement distribution over long distances [259,260].

It is likely that integrated and compact laser-cooled atomic systems will be advanced in parallel with solid-state quantum memories, in order to realize highly multiplexed quantum state storage. Further refinements in adapting optical cavities and atom–atom interactions in these systems are expected to overcome fundamental limitations associated with probabilistic entanglement creation schemes. In the long run, novel solid-state QOM materials will be integrated with photonic circuitry to realize fully integrated and scalable QOMs. We expect integrated QOM systems to initially operate at milli-Kelvin to Kelvin temperatures and perhaps high B-fields. Eventually, materials will be available to allow multiplexed operation at >1 K temperatures (and low B-fields) for large-scale operations (e.g., via efficient interfacing with telecom photons). Moreover, the implementation of multifunctional devices [47,261] in solid-state systems integrating quantum state generation, gate operation, storage, and non-destructive detection can open up possibilities for compact and scalable system design [262].

We also note that by using satellites, it is possible to establish a global quantum network that does not heavily rely on quantum repeater ideas. However, even in those settings, it may be advantageous to use quantum memories. For example, they would enable quantum communication between distant stations on Earth [3] or quantum teleportation over space-like separated nodes [263].

Funding. U.S. Department of Energy (3ERKJ381); Air Force Office of Scientific Research; National Science Foundation; National Research Council Canada.

Acknowledgment. Y.L. and M.H. acknowledge the support from U.S. Department of Energy, Office of Science, Office of Advanced Scientific Computing Research, through the Quantum Internet to Accelerate Scientific Discovery Program under Field Work Proposal 3ERKJ381. F.K.A. and C.S. acknowledge the High-Throughput Secure Networks challenge program of the National Research Council of Canada. A.K. acknowledges the support of the AFOSR and the NSF.

Disclosures. The authors declare no conflicts of interest.

Data availability. No data were generated or analyzed in this review paper.

REFERENCES

1. H. J. Kimble, "The quantum internet," Nature **453**, 1023–1030 (2008).
2. S. Wehner, D. Elkouss, and R. Hanson, "Quantum internet: a vision for the road ahead," Science **362**, eaam9288 (2018).
3. C. Simon, "Towards a global quantum network," Nat. Photonics **11**, 678–680 (2017).
4. S. Lloyd, J. H. Shapiro, F. N. Wong, P. Kumar, S. M. Shahriar, and H. P. Yuen, "Infrastructure for the quantum internet," ACM SIGCOMM Comput. Commun. Rev. **34**, 9–20 (2004).
5. H.-J. Briegel, W. Dür, J. I. Cirac, and P. Zoller, "Quantum repeaters: the role of imperfect local operations in quantum communication," Phys. Rev. Lett. **81**, 5932 (1998).
6. L.-M. Duan, M. D. Lukin, J. I. Cirac, and P. Zoller, "Long-distance quantum communication with atomic ensembles and linear optics," Nature **414**, 413–418 (2001).
7. N. Sangouard, C. Simon, H. De Riedmatten, and N. Gisin, "Quantum repeaters based on atomic ensembles and linear optics," Rev. Mod. Phys. **83**, 33 (2011).
8. S. Muralidharan, J. Kim, N. Lütkenhaus, M. D. Lukin, and L. Jiang, "Ultrafast and fault-tolerant quantum communication across long distances," Phys. Rev. Lett. **112**, 250501 (2014).
9. S. Muralidharan, L. Li, J. Kim, N. Lütkenhaus, M. D. Lukin, and L. Jiang, "Optimal architectures for long distance quantum communication," Sci. Rep. **6**, 20463 (2016).
10. F. Rozpędek, K. Noh, Q. Xu, S. Guha, and L. Jiang, "Quantum repeaters based on concatenated bosonic and discrete-variable quantum codes," npj Quantum Inf. **7**, 102 (2021).
11. K. Fukui, R. N. Alexander, and P. van Loock, "All-optical long-distance quantum communication with Gottesman-Kitaev-Preskill qubits," Phys. Rev. Res. **3**, 033118 (2021).

12. C. H. Bennett, G. Brassard, C. Crépeau, R. Jozsa, A. Peres, and W. K. Wootters, "Teleporting an unknown quantum state via dual classical and Einstein-Podolsky-Rosen channels," Phys. Rev. Lett. **70**, 1895 (1993).
13. D. Bouwmeester, J.-W. Pan, K. Mattle, M. Eibl, H. Weinfurter, and A. Zeilinger, "Experimental quantum teleportation," Nature **390**, 575–579 (1997).
14. P. Komar, E. M. Kessler, M. Bishof, L. Jiang, A. S. Sørensen, J. Ye, and M. D. Lukin, "A quantum network of clocks," Nat. Phys. **10**, 582–587 (2014).
15. D. Gottesman, T. Jennewein, and S. Croke, "Longer-baseline telescopes using quantum repeaters," Phys. Rev. Lett. **109**, 070503 (2012).
16. F. Kaneda and P. G. Kwiat, "High-efficiency single-photon generation via large-scale active time multiplexing," Sci. Adv. **5**, eaaw8586 (2019).
17. K. B. Dideriksen, R. Schmieg, M. Zugenmaier, and E. S. Polzik, "Room-temperature single-photon source with near-millisecond built-in memory," Nat. Commun. **12**, 3699 (2021).
18. F. Kaneda, F. Xu, J. Chapman, and P. G. Kwiat, "Quantum-memory-assisted multi-photon generation for efficient quantum information processing," Optica **4**, 1034–1037 (2017).
19. R. Chrapkiewicz, M. Dąbrowski, and W. Wasilewski, "High-capacity angularly multiplexed holographic memory operating at the single-photon level," Phys. Rev. Lett. **118**, 063603 (2017).
20. X. Han, W. Fu, C.-L. Zou, L. Jiang, and H. X. Tang, "Microwave-optical quantum frequency conversion," Optica **8**, 1050–1064 (2021).
21. M. Mazelanik, A. Leszczyński, M. Lipka, W. Wasilewski, and M. Parniak, "Real-time ghost imaging of Bell-nonlocal entanglement between a photon and a quantum memory," Quantum **5**, 493 (2021).
22. S. Zaiser, T. Rendler, I. Jakobi, T. Wolf, S.-Y. Lee, S. Wagner, V. Bergholm, T. Schulte-Herbrüggen, P. Neumann, and J. Wrachtrup, "Enhancing quantum sensing sensitivity by a quantum memory," Nat. Commun. **7**, 12279 (2016).
23. M. Hosseini, K. M. Beck, Y. Duan, W. Chen, and V. Vuletić, "Partially nondestructive continuous detection of individual traveling optical photons," Phys. Rev. Lett. **116**, 033602 (2016).
24. D. Niemietz, P. Farrera, S. Langenfeld, and G. Rempe, "Nondestructive detection of photonic qubits," Nature **591**, 570–574 (2021).
25. E. Knill, R. Laflamme, and G. J. Milburn, "A scheme for efficient quantum computation with linear optics," Nature **409**, 46–52 (2001).
26. J.-M. Mol, L. Esguerra, M. Meister, D. E. Bruschi, A. W. Schell, J. Wolters, and L. Wörner, "Quantum memories for fundamental science in space," Quantum Sci. Technol. **8**, 024006 (2023).
27. L.-M. Duan and H. Kimble, "Scalable photonic quantum computation through cavity-assisted interactions," Phys. Rev. Lett. **92**, 127902 (2004).
28. A. Reiserer, N. Kalb, G. Rempe, and S. Ritter, "A quantum gate between a flying optical photon and a single trapped atom," Nature **508**, 237–240 (2014).
29. T. Tiecke, J. D. Thompson, N. P. de Leon, L. Liu, V. Vuletić, and M. D. Lukin, "Nanophotonic quantum phase switch with a single atom," Nature **508**, 241–244 (2014).
30. C. Nguyen, D. Sukachev, M. Bhaskar, B. Machielse, D. Levonian, E. Knall, P. Stroganov, R. Riedinger, H. Park, M. Lončar, and M. D. Lukin, "Quantum network nodes based on diamond qubits with an efficient nanophotonic interface," Phys. Rev. Lett. **123**, 183602 (2019).
31. L.-M. Duan and C. Monroe, "Colloquium: Quantum networks with trapped ions," Rev. Mod. Phys. **82**, 1209 (2010).
32. K. Hammerer, A. S. Sørensen, and E. S. Polzik, "Quantum interface between light and atomic ensembles," Rev. Mod. Phys. **82**, 1041 (2010).
33. A. I. Lvovsky, B. C. Sanders, and W. Tittel, "Optical quantum memory," Nat. Photonics **3**, 706–714 (2009).
34. X.-L. Pang, A.-L. Yang, J.-P. Dou, H. Li, C.-N. Zhang, E. Poem, D. J. Saunders, H. Tang, J. Nunn, I. A. Walmsley, and X.-M. Jin, "A hybrid quantum memory–enabled network at room temperature," Sci. Adv. **6**, eaax1425 (2020).
35. V. Fiore, Y. Yang, M. C. Kuzyk, R. Barbour, L. Tian, and H. Wang, "Storing optical information as a mechanical excitation in a silica optomechanical resonator," Phys. Rev. Lett. **107**, 133601 (2011).
36. A. Wallucks, I. Marinković, B. Hensen, R. Stockill, and S. Gröblacher, "A quantum memory at telecom wavelengths," Nat. Phys. **16**, 772–777 (2020).
37. D. F. Phillips, A. Fleischhauer, A. Mair, R. L. Walsworth, and M. D. Lukin, "Storage of light in atomic vapor," Phys. Rev. Lett. **86**, 783 (2001).
38. C. Liu, Z. Dutton, C. H. Behroozi, and L. V. Hau, "Observation of coherent optical information storage in an atomic medium using halted light pulses," Nature **409**, 490–493 (2001).
39. A. Kuzmich, W. Bowen, A. Boozer, A. Boca, C. Chou, L.-M. Duan, and H. Kimble, "Generation of nonclassical photon pairs for scalable quantum communication with atomic ensembles," Nature **423**, 731–734 (2003).
40. B. Julsgaard, J. Sherson, J. I. Cirac, J. Fiurášek, and E. S. Polzik, "Experimental demonstration of quantum memory for light," Nature **432**, 482–486 (2004).
41. M. D. Eisaman, A. André, F. Massou, M. Fleischhauer, A. S. Zibrov, and M. D. Lukin, "Electromagnetically induced transparency with tunable single-photon pulses," Nature **438**, 837–841 (2005).
42. X.-H. Bao, A. Reingruber, P. Dietrich, J. Rui, A. Dück, T. Strassel, L. Li, N.-L. Liu, B. Zhao, and J.-W. Pan, "Efficient and long-lived quantum memory with cold atoms inside a ring cavity," Nat. Phys. **8**, 517–521 (2012).
43. M. Sabooni, Q. Li, S. Kröll, and L. Rippe, "Efficient quantum memory using a weakly absorbing sample," Phys. Rev. Lett. **110**, 133604 (2013).
44. L. Ma, X. Lei, J. Yan, R. Li, T. Chai, Z. Yan, X. Jia, C. Xie, and K. Peng, "High-performance cavity-enhanced quantum memory with warm atomic cell," Nat. Commun. **13**, 2368 (2022).
45. T. Zhong, J. M. Kindem, J. G. Bartholomew, J. Rochman, I. Craiciu, E. Miyazono, M. Bettinelli, E. Cavalli, V. Verma, S. W. Nam, F. Marsili, M. D. Shaw, A. D. Beyer, and A. Faraon, "Nanophotonic rare-earth quantum memory with optically controlled retrieval," Science **357**, 1392–1395 (2017).
46. I. Craiciu, M. Lei, J. Rochman, J. M. Kindem, J. G. Bartholomew, E. Miyazono, T. Zhong, N. Sinclair, and A. Faraon, "Nanophotonic quantum storage at telecommunication wavelength," Phys. Rev. Appl. **12**, 024062 (2019).
47. I. Craiciu, M. Lei, J. Rochman, J. G. Bartholomew, and A. Faraon, "Multifunctional on-chip storage at telecommunication wavelength for quantum networks," Optica **8**, 114–121 (2021).
48. B. Gouraud, D. Maxein, A. Nicolas, O. Morin, and J. Laurat, "Demonstration of a memory for tightly guided light in an optical nanofiber," Phys. Rev. Lett. **114**, 180503 (2015).
49. C. Sayrin, C. Clausen, B. Albrecht, P. Schneeweiss, and A. Rauschenbeutel, "Storage of fiber-guided light in a nanofiber-trapped ensemble of cold atoms," Optica **2**, 353–356 (2015).
50. N. V. Corzo, J. Raskop, A. Chandra, A. S. Sheremet, B. Gouraud, and J. Laurat, "Waveguide-coupled single collective excitation of atomic arrays," Nature **566**, 359–362 (2019).
51. M. F. Askarani, T. Lutz, V. B. Verma, M. D. Shaw, S. W. Nam, N. Sinclair, D. Oblak, and W. Tittel, "Storage and reemission of heralded telecommunication-wavelength photons using a crystal waveguide," Phys. Rev. Appl. **11**, 054056 (2019).
52. D.-C. Liu, P.-Y. Li, T.-X. Zhu, L. Zheng, J.-Y. Huang, Z.-Q. Zhou, C.-F. Li, and G.-C. Guo, "On-demand storage of photonic qubits at telecom wavelengths," Phys. Rev. Lett. **129**, 210501 (2022).
53. C. Couteau, "Spontaneous parametric down-conversion," Contemp. Phys. **59**, 291–304 (2018).
54. C. Chou, S. Polyakov, A. Kuzmich, and H. Kimble, "Single-photon generation from stored excitation in an atomic ensemble," Phys. Rev. Lett. **92**, 213601 (2004).
55. M. Fleischhauer and M. D. Lukin, "Dark-state polaritons in electromagnetically induced transparency," Phys. Rev. Lett. **84**, 5094 (2000).
56. A. L. Alexander, J. J. Longdell, M. J. Sellars, and N. B. Manson, "Photon echoes produced by switching electric fields," Phys. Rev. Lett. **96**, 043602 (2006).
57. N. Sangouard, C. Simon, M. Afzelius, and N. Gisin, "Analysis of a quantum memory for photons based on controlled reversible inhomogeneous broadening," Phys. Rev. A **75**, 032327 (2007).
58. G. Hetet, J. Longdell, A. Alexander, P. K. Lam, and M. Sellars, "Electro-optic quantum memory for light using two-level atoms," Phys. Rev. Lett. **100**, 023601 (2008).
59. D. Saunders, J. Munns, T. Champion, C. Qiu, K. Kaczmarek, E. Poem, P. Ledingham, I. Walmsley, and J. Nunn, "Cavity-enhanced room-temperature broadband Raman memory," Phys. Rev. Lett. **116**, 090501 (2016).

60. P. Michelberger, T. Champion, M. Sprague, K. Kaczmarek, M. Barbieri, X. Jin, D. England, W. Kolthammer, D. Saunders, J. Nunn, and I. A. Walmsley, "Interfacing GHz-bandwidth heralded single photons with a warm vapour Raman memory," New J. Phys. **17**, 043006 (2015).
61. J. Guo, X. Feng, P. Yang, Z. Yu, L. Chen, C.-H. Yuan, and W. Zhang, "Double-slit photoelectron interference in strong-field ionization of the neon dimer," Nat. Commun. **10**, 1 (2019).
62. M. Afzelius, C. Simon, H. De Riedmatten, and N. Gisin, "Multimode quantum memory based on atomic frequency combs," Phys. Rev. A **79**, 052329 (2009).
63. H. De Riedmatten, M. Afzelius, M. U. Staudt, C. Simon, and N. Gisin, "A solid-state light–matter interface at the single-photon level," Nature **456**, 773–777 (2008).
64. L. Li, Y. Dudin, and A. Kuzmich, "Entanglement between light and an optical atomic excitation," Nature **498**, 466–469 (2013).
65. L. Li and A. Kuzmich, "Quantum memory with strong and controllable Rydberg-level interactions," Nat. Commun. **7**, 13618 (2016).
66. A. V. Gorshkov, A. André, M. D. Lukin, and A. S. Sørensen, "Photon storage in Λ-type optically dense atomic media. II. Free-space model," Phys. Rev. A **76**, 033805 (2007).
67. M. O. Scully and M. S. Zubairy, *Quantum Optics* (1997).
68. A. V. Gorshkov, A. André, M. D. Lukin, and A. S. Sørensen, "Photon storage in Λ-type optically dense atomic media. I. Cavity model," Phys. Rev. A **76**, 033804 (2007).
69. M. Afzelius and C. Simon, "Impedance-matched cavity quantum memory," Phys. Rev. A **82**, 022310 (2010).
70. S. A. Moiseev, S. N. Andrianov, and F. F. Gubaidullin, "Efficient multimode quantum memory based on photon echo in an optimal QED cavity," Phys. Rev. A **82**, 022311 (2010).
71. M. Fleischhauer, A. Imamoglu, and J. P. Marangos, "Electromagnetically induced transparency: optics in coherent media," Rev. Mod. Phys. **77**, 633 (2005).
72. N. Lauk, C. O'Brien, and M. Fleischhauer, "Fidelity of photon propagation in electromagnetically induced transparency in the presence of four-wave mixing," Phys. Rev. A **88**, 013823 (2013).
73. E. Saglamyurek, T. Hrushevskyi, A. Rastogi, K. Heshami, and L. J. LeBlanc, "Coherent storage and manipulation of broadband photons via dynamically controlled Autler–Townes splitting," Nat. Photonics **12**, 774–782 (2018).
74. S. H. Autler and C. H. Townes, "Stark effect in rapidly varying fields," Phys. Rev. **100**, 703 (1955).
75. A. Rastogi, E. Saglamyurek, T. Hrushevskyi, S. Hubele, and L. J. LeBlanc, "Discerning quantum memories based on electromagnetically-induced-transparency and Autler-Townes-splitting protocols," Phys. Rev. A **100**, 012314 (2019).
76. K. Reim, J. Nunn, V. Lorenz, B. Sussman, K. Lee, N. Langford, D. Jaksch, and I. Walmsley, "Towards high-speed optical quantum memories," Nat. Photonics **4**, 218–221 (2010).
77. K. Reim, P. Michelberger, K. Lee, J. Nunn, N. Langford, and I. Walmsley, "Single-photon-level quantum memory at room temperature," Phys. Rev. Lett. **107**, 053603 (2011).
78. J. Nunn, I. Walmsley, M. Raymer, K. Surmacz, F. Waldermann, Z. Wang, and D. Jaksch, "Mapping broadband single-photon wave packets into an atomic memory," Phys. Rev. A **75**, 011401 (2007).
79. J. Nunn, J. Munns, S. Thomas, K. T. Kaczmarek, C. Qiu, A. Feizpour, E. Poem, B. Brecht, D. Saunders, P. M. Ledingham, D. V. Reddy, M. G. Raymer, and I. A. Walmsley, "Theory of noise suppression in Λ-type quantum memories by means of a cavity," Phys. Rev. A **96**, 012338 (2017).
80. A. V. Gorshkov, A. André, M. D. Lukin, and A. S. Sørensen, "Photon storage in Λ-type optically dense atomic media. III. Effects of inhomogeneous broadening," Phys. Rev. A **76**, 033806 (2007).
81. B. Lauritzen, J. Minář, H. De Riedmatten, M. Afzelius, N. Sangouard, C. Simon, and N. Gisin, "Telecommunication-wavelength solid-state memory at the single photon level," Phys. Rev. Lett. **104**, 080502 (2010).
82. M. P. Hedges, J. J. Longdell, Y. Li, and M. J. Sellars, "Efficient quantum memory for light," Nature **465**, 1052–1056 (2010).
83. M. Hosseini, B. M. Sparkes, G. Campbell, P. K. Lam, and B. C. Buchler, "High efficiency coherent optical memory with warm rubidium vapour," Nat. Commun. **2**, 174 (2011).
84. M. Hosseini, B. M. Sparkes, G. Hetet, J. J. Longdell, P. K. Lam, and B. C. Buchler, "Coherent optical pulse sequencer for quantum applications," Nature **461**, 241–245 (2009).
85. B. Sparkes, M. Hosseini, C. Cairns, D. Higginbottom, G. Campbell, P. K. Lam, and B. Buchler, "Precision spectral manipulation: a demonstration using a coherent optical memory," Phys. Rev. X **2**, 021011 (2012).
86. G. Campbell, O. Pinel, M. Hosseini, T. C. Ralph, B. Buchler, and P. K. Lam, "Configurable unitary transformations and linear logic gates using quantum memories," Phys. Rev. Lett. **113**, 063601 (2014).
87. J. Nunn, K. Reim, K. Lee, V. Lorenz, B. Sussman, I. Walmsley, and D. Jaksch, "Multimode memories in atomic ensembles," Phys. Rev. Lett. **101**, 260502 (2008).
88. B. Lauritzen, J. Minář, H. De Riedmatten, M. Afzelius, and N. Gisin, "Approaches for a quantum memory at telecommunication wavelengths," Phys. Rev. A **83**, 012318 (2011).
89. S. P. Horvath, M. K. Alqedra, A. Kinos, A. Walther, J. M. Dahlström, S. Kröll, and L. Rippe, "Noise-free on-demand atomic frequency comb quantum memory," Phys. Rev. Res **3**, 023099 (2021).
90. C. Liu, T.-X. Zhu, M.-X. Su, Y.-Z. Ma, Z.-Q. Zhou, C.-F. Li, and G.-C. Guo, "On-demand quantum storage of photonic qubits in an on-chip waveguide," Phys. Rev. Lett. **125**, 260504 (2020).
91. S. E. Beavan, P. M. Ledingham, J. J. Longdell, and M. J. Sellars, "Photon echo without a free induction decay in a double-Λ system," Opt. Lett. **36**, 1272–1274 (2011).
92. V. Damon, M. Bonarota, A. Louchet-Chauvet, T. Chaneliere, and J.-L. Le Gouët, "Revival of silenced echo and quantum memory for light," New J. Phys. **13**, 093031 (2011).
93. Y.-Z. Ma, M. Jin, D.-L. Chen, Z.-Q. Zhou, C.-F. Li, and G.-C. Guo, "Elimination of noise in optically rephased photon echoes," Nat. Commun. **12**, 4378 (2021).
94. A. Arcangeli, A. Ferrier, and P. Goldner, "Stark echo modulation for quantum memories," Phys. Rev. A **93**, 062303 (2016).
95. A. Fossati, S. Liu, J. Karlsson, A. Ikesue, A. Tallaire, A. Ferrier, D. Serrano, and P. Goldner, "A frequency-multiplexed coherent electro-optic memory in rare earth doped nanoparticles," Nano Lett. **20**, 7087–7093 (2020).
96. A. M. Marino, R. C. Pooser, V. Boyer, and P. D. Lett, "Tunable delay of Einstein–Podolsky–Rosen entanglement," Nature **457**, 859–862 (2009).
97. K. Kaczmarek, P. Ledingham, B. Brecht, S. Thomas, G. Thekkadath, O. Lazo-Arjona, J. Munns, E. Poem, A. Feizpour, D. Saunders, J. Nunn, and I. A. Walmsley, "High-speed noise-free optical quantum memory," Phys. Rev. A **97**, 042316 (2018).
98. S. Thomas, S. Sagona-Stophel, Z. Schofield, I. Walmsley, and P. Ledingham, "A single-photon-compatible telecom-c-band quantum memory in a hot atomic gas," arXiv, arXiv:2211.04415 (2022).
99. R. Finkelstein, E. Poem, O. Michel, O. Lahad, and O. Firstenberg, "Fast, noise-free memory for photon synchronization at room temperature," Sci. Adv. **4**, eaap8598 (2018).
100. O. Davidson, O. Yogev, E. Poem, and O. Firstenberg, "Fast, noise-free atomic optical memory with 35-percent end-to-end efficiency," Commun. Phys. **6**, 131 (2023).
101. B. Julsgaard, A. Kozhekin, and E. S. Polzik, "Experimental long-lived entanglement of two macroscopic objects," Nature **413**, 400–403 (2001).
102. O. Katz, R. Shaham, and O. Firstenberg, "Coupling light to a nuclear spin gas with a two-photon linewidth of five millihertz," Sci. Adv. **7**, eabe9164 (2021).
103. O. Katz, R. Shaham, E. Reches, A. V. Gorshkov, and O. Firstenberg, "Optical quantum memory for noble-gas spins based on spin-exchange collisions," Phys. Rev. A **105**, 042606 (2022).
104. R. Shaham, O. Katz, and O. Firstenberg, "Strong coupling of alkali-metal spins to noble-gas spins with an hour-long coherence time," Nat. Phys. **18**, 506–510 (2022).
105. Y. Yu, F. Ma, X.-Y. Luo, B. Jing, P.-F. Sun, R.-Z. Fang, C.-W. Yang, H. Liu, M.-Y. Zheng, X.-P. Xie, W.-J. Zhang, L.-X. You, Z. Wang, T.-Y. Chen, Q. Zhang, X.-H. Bao, and J.-W. Pan, "Entanglement of two quantum memories via fibres over dozens of kilometers," Nature **578**, 240–245 (2020).
106. M. K. Bhaskar, R. Riedinger, B. Machielse, D. S. Levonian, C. T. Nguyen, E. N. Knall, H. Park, D. Englund, M. Lončar, D. D. Sukachev, and M. D. Lukin, "Experimental demonstration of memory-enhanced quantum communication," Nature **580**, 60–64 (2020).
107. B. Hacker, S. Welte, G. Rempe, and S. Ritter, "A photon–photon quantum gate based on a single atom in an optical resonator," Nature **536**, 193–196 (2016).

108. S. Sun, H. Kim, Z. Luo, G. S. Solomon, and E. Waks, "A single-photon switch and transistor enabled by a solid-state quantum memory," Science **361**, 57–60 (2018).
109. C.-W. Chou, J. Laurat, H. Deng, K. S. Choi, H. De Riedmatten, D. Felinto, and H. J. Kimble, "Functional quantum nodes for entanglement distribution over scalable quantum networks," Science **316**, 1316–1320 (2007).
110. C. Simon and W. T. Irvine, "Robust long-distance entanglement and a loophole-free bell test with ions and photons," Phys. Rev. Lett. **91**, 110405 (2003).
111. L.-M. Duan and H. Kimble, "Efficient engineering of multiatom entanglement through single-photon detections," Phys. Rev. Lett. **90**, 253601 (2003).
112. X.-L. Feng, Z.-M. Zhang, X.-D. Li, S.-Q. Gong, and Z.-Z. Xu, "Entangling distant atoms by interference of polarized photons," Phys. Rev. Lett. **90**, 217902 (2003).
113. S. D. Barrett and P. Kok, "Efficient high-fidelity quantum computation using matter qubits and linear optics," Phys. Rev. A **71**, 060310 (2005).
114. B. Hensen, H. Bernien, A. E. Dréau, A. Reiserer, N. Kalb, M. S. Blok, J. Ruitenberg, R. F. Vermeulen, R. N. Schouten, C. Abellán, W. Amaya, V. Pruneri, M. W. Mitchell, M. Markham, D. J. Twitchen, D. Elkouss, S. Wehner, T. H. Taminiau, and R. Hanson, "Loophole-free Bell inequality violation using electron spins separated by 1.3 kilometres," Nature **526**, 682–686 (2015).
115. H. Tanji-Suzuki, I. D. Leroux, M. H. Schleier-Smith, M. Cetina, A. T. Grier, J. Simon, and V. Vuletić, "Interaction between atomic ensembles and optical resonators: Classical description," in *Advances in Atomic, Molecular, and Optical Physics* (Elsevier, 2011), Vol. **60**, pp. 201–237.
116. T. Wilk, S. C. Webster, A. Kuhn, and G. Rempe, "Single-atom single-photon quantum interface," Science **317**, 488–490 (2007).
117. M. D. Lukin, M. Fleischhauer, R. Cote, L. Duan, D. Jaksch, J. I. Cirac, and P. Zoller, "Dipole blockade and quantum information processing in mesoscopic atomic ensembles," Phys. Rev. Lett. **87**, 037901 (2001).
118. M. Saffman and T. Walker, "Creating single-atom and single-photon sources from entangled atomic ensembles," Phys. Rev. A **66**, 065403 (2002).
119. F. Bariani, Y. Dudin, T. Kennedy, and A. Kuzmich, "Dephasing of multiparticle Rydberg excitations for fast entanglement generation," Phys. Rev. Lett. **108**, 030501 (2012).
120. Y. Dudin and A. Kuzmich, "Strongly interacting Rydberg excitations of a cold atomic gas," Science **336**, 887–889 (2012).
121. H. Busche, P. Huillery, S. W. Ball, T. Ilieva, M. P. Jones, and C. S. Adams, "Contactless nonlinear optics mediated by long-range Rydberg interactions," Nat. Phys. **13**, 655–658 (2017).
122. F. Ripka, H. Kubler, R. Low, and T. Pfau, "A room-temperature single-photon source based on strongly interacting Rydberg atoms," Science **362**, 446–449 (2018).
123. D. P. Ornelas-Huerta, A. N. Craddock, E. A. Goldschmidt, A. J. Hachtel, Y. Wang, P. Bienias, A. V. Gorshkov, S. L. Rolston, and J. V. Porto, "On-demand indistinguishable single photons from an efficient and pure source based on a Rydberg ensemble," Optica **7**, 813–819 (2020).
124. Y. Wang, J. Li, S. Zhang, K. Su, Y. Zhou, K. Liao, S. Du, H. Yan, and S.-L. Zhu, "Efficient quantum memory for single-photon polarization qubits," Nat. Photonics **13**, 346–351 (2019).
125. Y. Dudin, L. Li, and A. Kuzmich, "Light storage on the time scale of a minute," Phys. Rev. A **87**, 031801 (2013).
126. C. Simon, H. De Riedmatten, M. Afzelius, N. Sangouard, H. Zbinden, and N. Gisin, "Quantum repeaters with photon pair sources and multimode memories," Phys. Rev. Lett. **98**, 190503 (2007).
127. O. Collins, S. Jenkins, A. Kuzmich, and T. Kennedy, "Multiplexed memory-insensitive quantum repeaters," Phys. Rev. Lett. **98**, 060502 (2007).
128. P. Jobez, C. Laplane, N. Timoney, N. Gisin, A. Ferrier, P. Goldner, and M. Afzelius, "Coherent spin control at the quantum level in an ensemble-based optical memory," Phys. Rev. Lett. **114**, 230502 (2015).
129. M. Zhong, M. P. Hedges, R. L. Ahlefeldt, J. G. Bartholomew, S. E. Beavan, S. M. Wittig, J. J. Longdell, and M. J. Sellars, "Optically addressable nuclear spins in a solid with a six-hour coherence time," Nature **517**, 177–180 (2015).
130. H. Y. Carr and E. M. Purcell, "Effects of diffusion on free precession in nuclear magnetic resonance experiments," Phys. Rev. **94**, 630 (1954).
131. S. Meiboom and D. Gill, "Modified spin-echo method for measuring nuclear relaxation times," Rev. Sci. Instrum. **29**, 688–691 (1958).
132. P. Siyushev, K. Xia, R. Reuter, M. Jamali, N. Zhao, N. Yang, C. Duan, N. Kukharchyk, A. Wieck, R. Kolesov, and J. Wrachtrup, "Coherent properties of single rare-earth spin qubits," Nat. Commun. **5**, 3895 (2014).
133. A. M. Souza, G. A. Alvarez, and D. Suter, "Robust dynamical decoupling for quantum computing and quantum memory," Phys. Rev. Lett. **106**, 240501 (2011).
134. F. K. Asadi, S. Wein, and C. Simon, "Protocols for long-distance quantum communication with single ^{167}Er ions," Quantum Sci. Technol. **5**, 045015 (2020).
135. K. Boone, J.-P. Bourgoin, E. Meyer-Scott, K. Heshami, T. Jennewein, and C. Simon, "Entanglement over global distances via quantum repeaters with satellite links," Phys. Rev. A **91**, 052325 (2015).
136. K. De Greve, L. Yu, P. L. McMahon, J. S. Pelc, C. M. Natarajan, N. Y. Kim, E. Abe, S. Maier, C. Schneider, M. Kamp, S. Höfling, R. H. Hadfield, A. Forchel, M. M. Fejer, and Y. Yamamoto, "Quantum-dot spin–photon entanglement via frequency downconversion to telecom wavelength," Nature **491**, 421–425 (2012).
137. N. Lauk, N. Sinclair, S. Barzanjeh, J. P. Covey, M. Saffman, M. Spiropulu, and C. Simon, "Perspectives on quantum transduction," Quantum Sci. Technol. **5**, 020501 (2020).
138. F. K. Asadi, J.-W. Ji, and C. Simon, "Proposal for transduction between microwave and optical photons using ^{167}Er-doped yttrium orthosilicate," Phys. Rev. A **105**, 062608 (2022).
139. J.-Y. Chen, C. Tang, Z.-H. Ma, Z. Li, Y. M. Sua, and Y.-P. Huang, "Efficient and highly tunable second-harmonic generation in Z-cut periodically poled lithium niobate nanowaveguides," Opt. Lett. **45**, 3789–3792 (2020).
140. B. Albrecht, P. Farrera, X. Fernandez-Gonzalvo, M. Cristiani, and H. De Riedmatten, "A waveguide frequency converter connecting rubidium-based quantum memories to the telecom C-band," Nat. Commun. **5**, 3376 (2014).
141. M. Allgaier, V. Ansari, L. Sansoni, C. Eigner, V. Quiring, R. Ricken, G. Harder, B. Brecht, and C. Silberhorn, "Highly efficient frequency conversion with bandwidth compression of quantum light," Nat. Commun. **8**, 14288 (2017).
142. C. L. Morrison, M. Rambach, Z. X. Koong, F. Graffitti, F. Thorburn, A. K. Kar, Y. Ma, S.-I. Park, J. D. Song, N. G. Stoltz, D. Bouwmeester, A. Fedrizzi, and B. D. Gerardot, "A bright source of telecom single photons based on quantum frequency conversion," Appl. Phys. Lett. **118**, 174003 (2021).
143. A. Dréau, A. Tchebotareva, A. El Mahdaoui, C. Bonato, and R. Hanson, "Quantum frequency conversion of single photons from a nitrogen-vacancy center in diamond to telecommunication wavelengths," Phys. Rev. Appl. **9**, 064031 (2018).
144. T. Walker, K. Miyanishi, R. Ikuta, H. Takahashi, S. V. Kashanian, Y. Tsujimoto, K. Hayasaka, T. Yamamoto, N. Imoto, and M. Keller, "Long-distance single photon transmission from a trapped ion via quantum frequency conversion," Phys. Rev. Lett. **120**, 203601 (2018).
145. M. Bock, P. Eich, S. Kucera, M. Kreis, A. Lenhard, C. Becher, and J. Eschner, "High-fidelity entanglement between a trapped ion and a telecom photon via quantum frequency conversion," Nat. Commun. **9**, 1998 (2018).
146. J. V. Rakonjac, D. Lago-Rivera, A. Seri, M. Mazzera, S. Grandi, and H. de Riedmatten, "Entanglement between a telecom photon and an on-demand multimode solid-state quantum memory," Phys. Rev. Lett. **127**, 210502 (2021).
147. D. Lago-Rivera, S. Grandi, J. V. Rakonjac, A. Seri, and H. de Riedmatten, "Entanglement between a telecom photon and an on-demand multimode solid-state quantum memory," Nature **594**, 37–40 (2021).
148. T.-S. Yang, Z.-Q. Zhou, Y.-L. Hua, X. Liu, Z.-F. Li, P.-Y. Li, Y. Ma, C. Liu, P.-J. Liang, X. Li, Y.-X. Xiao, J. Hu, C.-F. Li, and G.-C. Guo, "Multiplexed storage and real-time manipulation based on a multiple degree-of-freedom quantum memory," Nat. Commun. **9**, 3407 (2018).
149. S.-Y. Lan, A. Radnaev, O. Collins, D. Matsukevich, T. Kennedy, and A. Kuzmich, "A multiplexed quantum memory," Opt. Express **17**, 13639–13645 (2009).
150. Y. Pu, N. Jiang, W. Chang, H. Yang, C. Li, and L. Duan, "Experimental realization of a multiplexed quantum memory with 225 individually accessible memory cells," Nat. Commun. **8**, 15359 (2017).
151. L. Heller, P. Farrera, G. Heinze, and H. de Riedmatten, "Cold-atom temporally multiplexed quantum memory with cavity-enhanced noise suppression," Phys. Rev. Lett. **124**, 210504 (2020).

152. M. Parniak, M. Dąbrowski, M. Mazelanik, A. Leszczyński, M. Lipka, and W. Wasilewski, "Wavevector multiplexed atomic quantum memory via spatially-resolved single-photon detection," Nat. Commun. **8**, 2140 (2017).
153. L. Tian, Z. Xu, L. Chen, W. Ge, H. Yuan, Y. Wen, S. Wang, S. Li, and H. Wang, "Wavevector multiplexed atomic quantum memory via spatially-resolved single-photon detection,' Phys. Rev. Lett. **119**, 130505 (2017).
154. A. Nicolas, L. Veissier, L. Giner, E. Giacobino, D. Maxein, and J. Laurat, "A quantum memory for orbital angular momentum photonic qubits," Nat. Photonics **8**, 234–238 (2014).
155. V. Parigi, V. D'Ambrosio, C. Arnold, L. Marrucci, F. Sciarrino, and J. Laurat, "Storage and retrieval of vector beams of light in a multiple-degree-of-freedom quantum memory," Nat. Commun. **6**, 7706 (2015).
156. A. Seri, D. Lago-Rivera, A. Lenhard, G. Corrielli, R. Osellame, M. Mazzera, and H. de Riedmatten, "Quantum storage of frequency-multiplexed heralded single photons," Phys. Rev. Lett. **123**, 080502 (2019).
157. M. Gündoğan, P. M. Ledingham, A. Almasi, M. Cristiani, and H. De Riedmatten, "Quantum storage of a photonic polarization qubit in a solid," Phys. Rev. Lett. **108**, 190504 (2012).
158. J.-S. Tang, Z.-Q. Zhou, Y.-T. Wang, Y.-L. Li, X. Liu, Y.-L. Hua, Y. Zou, S. Wang, D.-Y. He, G. Chen, Y.-N. Sun, Y. Yu, M.-F. Li, G.-W. Zha, H.-Q. Ni, Z.-C. Niu, C.-F. Li, and G.-C. Guo, "Storage of multiple single-photon pulses emitted from a quantum dot in a solid-state quantum memory," Nat. Commun. **6**, 8652 (2015).
159. M. Businger, L. Nicolas, T. S. Mejia, A. Ferrier, P. Goldner, and M. Afzelius, "Non-classical correlations over 1250 modes between telecom photons and 979-nm photons stored in $^{171}Yb^{3+}$:Y_2SiO_5," Nat. Commun. **13**, 6438 (2022).
160. S.-H. Wei, B. Jing, X.-Y. Zhang, J.-Y. Liao, H. Li, L.-X. You, Z. Wang, Y. Wang, G.-W. Deng, H.-Z. Song, D. Oblak, G.-C. Guo, and Q. Zhou, "Quantum storage of 1650 modes of single photons at telecom wavelength," arXiv, arXiv:2209.00802 (2022).
161. N. Sinclair, E. Saglamyurek, H. Mallahzadeh, J. A. Slater, M. George, R. Ricken, M. P. Hedges, D. Oblak, C. Simon, W. Sohler, and W. Tittel, "Spectral multiplexing for scalable quantum photonics using an atomic frequency comb quantum memory and feed-forward control," Phys. Rev. Lett. **113**, 053603 (2014).
162. C.-W. Chou, H. De Riedmatten, D. Felinto, S. V. Polyakov, S. J. Van Enk, and H. J. Kimble, "Measurement-induced entanglement for excitation stored in remote atomic ensembles," Nature **438**, 828–832 (2005).
163. K. S. Choi, H. Deng, J. Laurat, and H. Kimble, "Mapping photonic entanglement into and out of a quantum memory," Nature **452**, 67–71 (2008).
164. S. Ritter, C. Nölleke, C. Hahn, A. Reiserer, A. Neuzner, M. Uphoff, M. Mücke, E. Figueroa, J. Bochmann, and G. Rempe, "An elementary quantum network of single atoms in optical cavities," Nature **484**, 195–200 (2012).
165. B. Jing, X.-J. Wang, Y. Yu, P.-F. Sun, Y. Jiang, S.-J. Yang, W.-H. Jiang, X.-Y. Luo, J. Zhang, X. Jiang, X.-H. Bao, and J.-W. Pan, "Entanglement of three quantum memories via interference of three single photons," Nat. Photonics **13**, 210–213 (2019).
166. Y.-A. Chen, Q. Zhang, and T.-Y. Chen, "An integrated space-to-ground quantum communication network over 4,600 kilometres," Nature **589**, 214–219 (2021).
167. S. Wengerowsky, S. K. Joshi, F. Steinlechner, H. Hübel, and R. Ursin, "An entanglement-based wavelength-multiplexed quantum communication network," Nature **564**, 225–228 (2018).
168. S. K. Joshi, D. Aktas, S. Wengerowsky, M. Lončarić, S. P. Neumann, B. Liu, T. Scheidl, G. C. Lorenzo, Ž. Samec, L. Kling, A. Qiu, M. Razavi, M. Stipčević, J. G. Rarity, and R. Ursin, "A trusted node–free eight-user metropolitan quantum communication network," Sci. Adv. **6**, eaba0959 (2020).
169. X. Liu, J. Hu, Z.-F. Li, X. Li, P.-Y. Li, P.-J. Liang, Z.-Q. Zhou, C.-F. Li, and G.-C. Guo, "Heralded entanglement distribution between two absorptive quantum memories," Nature **594**, 41–45 (2021).
170. M. Pompili, S. L. Hermans, S. Baier, H. K. Beukers, P. C. Humphreys, R. N. Schouten, R. F. Vermeulen, M. J. Tiggelman, L. dos Santos Martins, B. Dirkse, S. Wehner, and R. Hanson, "Realization of a multinode quantum network of remote solid-state qubits," Science **372**, 259–264 (2021).
171. N. Maring, P. Farrera, K. Kutluer, M. Mazzera, G. Heinze, and H. de Riedmatten, "Photonic quantum state transfer between a cold atomic gas and a crystal," Nature **551**, 485–488 (2017).
172. S. Hermans, M. Pompili, H. Beukers, S. Baier, J. Borregaard, and R. Hanson, "Qubit teleportation between non-neighbouring nodes in a quantum network," Nature **605**, 663–668 (2022).
173. D. D. Sukachev, A. Sipahigil, C. T. Nguyen, M. K. Bhaskar, R. E. Evans, F. Jelezko, and M. D. Lukin, "Silicon-vacancy spin qubit in diamond: a quantum memory exceeding 10 ms with single-shot state readout," Phys. Rev. Lett. **119**, 223602 (2017).
174. C. E. Bradley, J. Randall, M. H. Abobeih, R. Berrevoets, M. Degen, M. A. Bakker, M. Markham, D. Twitchen, and T. H. Taminiau, "A ten-qubit solid-state spin register with quantum memory up to one minute," Phys. Rev. X **9**, 031045 (2019).
175. E. Saglamyurek, J. Jin, V. B. Verma, M. D. Shaw, F. Marsili, S. W. Nam, D. Oblak, and W. Tittel, "Quantum storage of entangled telecom-wavelength photons in an erbium-doped optical fibre," Nat. Photonics **9**, 83–87 (2015).
176. J. S. Stuart, M. Hedges, R. Ahlefeldt, and M. Sellars, "Initialization protocol for efficient quantum memories using resolved hyperfine structure," Phys. Rev. Res. **3**, L032054 (2021).
177. S. Duranti, S. Wengerowsky, L. Feldmann, A. Seri, B. Casabone, and H. de Riedmatten, "Efficient cavity-assisted storage of photonic qubits in a solid-state quantum memory," arXiv, arXiv:2307.03509 (2023).
178. A. Ortu, A. Holzäpfel, J. Etesse, and M. Afzelius, "Storage of photonic time-bin qubits for up to 20 ms in a rare-earth doped crystal," npj Quantum Inf. **8**, 29 (2022).
179. P. Vernaz-Gris, K. Huang, M. Cao, A. S. Sheremet, and J. Laurat, "Highly-efficient quantum memory for polarization qubits in a spatially-multiplexed cold atomic ensemble," Nat. Commun. **9**, 363 (2018).
180. M. Cao, F. Hoffet, S. Qiu, A. S. Sheremet, and J. Laurat, "Efficient reversible entanglement transfer between light and quantum memories," Optica **7**, 1440–1444 (2020).
181. X.-J. Wang, S.-J. Yang, P.-F. Sun, B. Jing, J. Li, M.-T. Zhou, X.-H. Bao, and J.-W. Pan, "Cavity-enhanced atom-photon entanglement with subsecond lifetime," Phys. Rev. Lett. **126**, 090501 (2021).
182. G. Buser, R. Mottola, B. Cotting, J. Wolters, and P. Treutlein, "Single-photon storage in a ground-state vapor cell quantum memory," PRX Quantum **3**, 020349 (2022).
183. O. Davidson, O. Yogev, E. Poem, and O. Firstenberg, "Single-photon synchronization with a room-temperature atomic quantum memory," Phys. Rev. Lett. **131**, 033601 (2023).
184. A. Ortu, J. V. Rakonjac, A. Holzäpfel, A. Seri, S. Grandi, M. Mazzera, H. de Riedmatten, and M. Afzelius, "Multimode capacity of atomic-frequency comb quantum memories," Quantum Sci. Technol. **7**, 035024 (2022).
185. M. F. Askarani, A. Das, J. H. Davidson, G. C. Amaral, N. Sinclair, J. A. Slater, S. Marzban, C. W. Thiel, R. L. Cone, D. Oblak, and W. Tittel, "Long-lived solid-state optical memory for high-rate quantum repeaters," Phys. Rev. Lett. **127**, 220502 (2021).
186. M. Businger, A. Tiranov, K. T. Kaczmarek, S. Welinski, Z. Zhang, A. Ferrier, P. Goldner, and M. Afzelius, "Optical spin-wave storage in a solid-state hybridized electron-nuclear spin ensemble," Phys. Rev. Lett. **124**, 053606 (2020).
187. Y. Ma, Y.-Z. Ma, Z.-Q. Zhou, C.-F. Li, and G.-C. Guo, "One-hour coherent optical storage in an atomic frequency comb memory," Nat. Commun. **12**, 2381 (2021).
188. A. Delteil, Z. Sun, W.-B. Gao, E. Togan, S. Faelt, and A. Imamoğlu, "Generation of heralded entanglement between distant hole spins," Nat. Phys. **12**, 218–223 (2016).
189. R. Stockill, M. Stanley, L. Huthmacher, E. Clarke, M. Hugues, A. Miller, C. Matthiesen, C. Le Gall, and M. Atatüre, "Phase-tuned entangled state generation between distant spin qubits," Phys. Rev. Lett. **119**, 010503 (2017).
190. J. V. Rakonjac, S. Grandi, S. Wengerowsky, D. Lago-Rivera, F. Appas, and H. de Riedmatten, "Transmission of light-matter entanglement over a metropolitan network," arXiv, arXiv:2304.05416 (2023).
191. V. Krutyanskiy, M. Galli, V. Krcmarsky, S. Baier, D. Fioretto, Y. Pu, A. Mazloom, P. Sekatski, M. Canteri, M. Teller, J. Schupp, J. Bate, M. Meraner, N. Sangouard, B. P. Lanyon, and T. E. Northup, "Entanglement of trapped-ion qubits separated by 230 meters," Phys. Rev. Lett. **130**, 050803 (2023).

192. V. Krutyanskiy, M. Meraner, J. Schupp, V. Krcmarsky, H. Hainzer, and B. Lanyon, "Light-matter entanglement over 50 km of optical fibre," npj Quantum Inf. **5**, 72 (2019).
193. T. van Leent, M. Bock, F. Fertig, R. Garthoff, S. Eppelt, Y. Zhou, P. Malik, M. Seubert, T. Bauer, W. Rosenfeld, W. Zhang, C. Becher, and H. Weinfurter, "Entangling single atoms over 33 km telecom fibre," Nature **607**, 69–73 (2022).
194. H. Li, J.-P. Dou, X.-L. Pang, T.-H. Yang, C.-N. Zhang, Y. Chen, J.-M. Li, I. A. Walmsley, and X.-M. Jin, "Heralding quantum entanglement between two room-temperature atomic ensembles," Optica **8**, 925–929 (2021).
195. E. Saglamyurek, N. Sinclair, J. Jin, J. A. Slater, D. Oblak, F. Bussieres, M. George, R. Ricken, W. Sohler, and W. Tittel, "Broadband waveguide quantum memory for entangled photons," Nature **469**, 512–515 (2011).
196. Y.-F. Hsiao, P.-J. Tsai, H.-S. Chen, S.-X. Lin, C.-C. Hung, C.-H. Lee, Y.-H. Chen, Y.-F. Chen, A. Y. Ite, and Y.-C. Chen, "Highly efficient coherent optical memory based on electromagnetically induced transparency," Phys. Rev. Lett. **120**, 183602 (2018).
197. W. Chang, C. Li, Y.-K. Wu, N. Jiang, S. Zhang, Y.-F. Pu, X.-Y. Chang, and L.-M. Duan, "Long-distance entanglement between a multiplexed quantum memory and a telecom photon," Phys. Rev. X **9**, 041033 (2019).
198. I. Novikova, A. V. Gorshkov, D. F. Phillips, A. S. Sørensen, M. D. Lukin, and R. L. Walsworth, "Optimal control of light pulse storage and retrieval," Phys. Rev. Lett. **98**, 243602 (2007).
199. I. Novikova, N. B. Phillips, and A. V. Gorshkov, "Optimal light storage with full pulse-shape control," Phys. Rev. A **78**, 021802 (2008).
200. N. B. Phillips, A. V. Gorshkov, and I. Novikova, "Optimal light storage in atomic vapor," Phys. Rev. A **78**, 023801 (2008).
201. O. Katz and O. Firstenberg, "Light storage for one second in room-temperature alkali vapor," Nat. Commun. **9**, 2074 (2018).
202. S. E. Thomas, T. M. Hird, J. H. Munns, B. Brecht, D. J. Saunders, J. Nunn, I. A. Walmsley, and P. M. Ledingham, "Raman quantum memory with built-in suppression of four-wave-mixing noise," Phys. Rev. A **100**, 033801 (2019).
203. E. Saglamyurek, T. Hrushevskyi, A. Rastogi, L. Cooke, B. D. Smith, and L. J. LeBlanc, "Storing short single-photon-level optical pulses in Bose–Einstein condensates for high-performance quantum memory," New J. Phys. **23**, 043028 (2021).
204. D. B. Higginbottom, F. K. Asadi, C. Chartrand, J.-W. Ji, L. Bergeron, M. L. Thewalt, C. Simon, and S. Simmons, "Memory and transduction prospects for silicon T centre devices," arXiv, arXiv:2209.11731 (2022).
205. M. Hosseini, G. Campbell, B. M. Sparkes, P. K. Lam, and B. C. Buchler, "Unconditional room temperature quantum memory," Nat. Phys. **7**, 794–798 (2011).
206. Y.-W. Cho, G. Campbell, J. Everett, J. Bernu, D. Higginbottom, M. Cao, J. Geng, N. Robins, P. Lam, and B. Buchler, "Highly efficient optical quantum memory with long coherence time in cold atoms," Optica **3**, 100–107 (2016).
207. Z.-Q. Zhou, W.-B. Lin, M. Yang, C.-F. Li, and G.-C. Guo, "Realization of reliable solid-state quantum memory for photonic polarization qubit," Phys. Rev. Lett. **108**, 190505 (2012).
208. M. Gündoğan, P. M. Ledingham, K. Kutluer, M. Mazzera, and H. De Riedmatten, "Solid state spin-wave quantum memory for time-bin qubits," Phys. Rev. Lett. **114**, 230501 (2015).
209. T. Böttger, C. Thiel, R. Cone, and Y. Sun, "Effects of magnetic field orientation on optical decoherence in Er^{3+}:Y_2SiO_5," Phys. Rev. B **79**, 115104 (2009).
210. M. Rančić, M. P. Hedges, R. L. Ahlefeldt, and M. J. Sellars, "Coherence time of over a second in a telecom-compatible quantum memory storage material," Nat. Phys. **14**, 50–54 (2018).
211. J. H. Davidson, P. Lefebvre, J. Zhang, D. Oblak, and W. Tittel, "Improved light-matter interaction for storage of quantum states of light in a thulium-doped crystal cavity," Phys. Rev. A **101**, 042333 (2020).
212. M.-H. Jiang, W. Xue, Q. He, Y.-Y. An, X. Zheng, W.-J. Xu, Y.-B. Xie, Y. Lu, S. Zhu, and X.-S. Ma, "Quantum storage of entangled photons at telecom wavelengths in a crystal," Nat. Commun. **14**, 6995 (2023).
213. A. Radnaev, Y. Dudin, R. Zhao, H. Jen, S. Jenkins, A. Kuzmich, and T. Kennedy, "A quantum memory with telecom-wavelength conversion," Nat. Phys. **6**, 894–899 (2010).
214. S.-J. Yang, X.-J. Wang, X.-H. Bao, and J.-W. Pan, "An efficient quantum light–matter interface with sub-second lifetime," Nat. Photonics **10**, 381–384 (2016).
215. P. C. Humphreys, N. Kalb, J. P. Morits, R. N. Schouten, R. F. Vermeulen, D. J. Twitchen, M. Markham, and R. Hanson, "Deterministic delivery of remote entanglement on a quantum network," Nature **558**, 268–273 (2018).
216. J. Hofmann, M. Krug, N. Ortegel, L. Gérard, M. Weber, W. Rosenfeld, and H. Weinfurter, "Heralded entanglement between widely separated atoms," Science **337**, 72–75 (2012).
217. J. Hannegan, J. D. Siverns, and Q. Quraishi, "Entanglement between a trapped-ion qubit and a 780-nm photon via quantum frequency conversion," Phys. Rev. A **106**, 042441 (2022).
218. Z.-S. Yuan, Y.-A. Chen, B. Zhao, S. Chen, J. Schmiedmayer, and J.-W. Pan, "Experimental demonstration of a BDCZ quantum repeater node," Nature **454**, 1098–1101 (2008).
219. V. Krutyanskiy, M. Canteri, M. Meraner, J. Bate, V. Krcmarsky, J. Schupp, N. Sangouard, and B. P. Lanyon, "A telecom-wavelength quantum repeater node based on a trapped-ion processor," Phys. Rev. Lett. **130**, 213601 (2023).
220. J. Schupp, V. Krcmarsky, V. Krutyanskiy, M. Meraner, T. Northup, and B. Lanyon, "Interface between trapped-ion qubits and traveling photons with close-to-optimal efficiency," PRX Quantum **2**, 020331 (2021).
221. K. Sharman, F. K. Asadi, S. C. Wein, and C. Simon, "Quantum repeaters based on individual electron spins and nuclear-spin-ensemble memories in quantum dots," Quantum **5**, 570 (2021).
222. F. K. Asadi, N. Lauk, S. Wein, N. Sinclair, C. O'Brien, and C. Simon, "Quantum repeaters with individual rare-earth ions at telecommunication wavelengths," Quantum **2**, 93 (2018).
223. C. Laplane, P. Jobez, J. Etesse, N. Gisin, and M. Afzelius, "Multimode and long-lived quantum correlations between photons and spins in a crystal," Phys. Rev. Lett. **118**, 210501 (2017).
224. K. Kutluer, M. Mazzera, and H. de Riedmatten, "Solid-state source of nonclassical photon pairs with embedded multimode quantum memory," Phys. Rev. Lett. **118**, 210502 (2017).
225. W. Rosenfeld, D. Burchardt, R. Garthoff, K. Redeker, N. Ortegel, M. Rau, and H. Weinfurter, "Event-ready bell test using entangled atoms simultaneously closing detection and locality loopholes," Phys. Rev. Lett. **119**, 010402 (2017).
226. A. D. Boozer, A. Boca, R. Miller, T. E. Northup, and H. J. Kimble, "Reversible state transfer between light and a single trapped atom," Phys. Rev. Lett. **98**, 193601 (2007).
227. H. P. Specht, C. Nölleke, A. Reiserer, M. Uphoff, E. Figueroa, S. Ritter, and G. Rempe, "A single-atom quantum memory," Nature **473**, 190–193 (2011).
228. B. Hacker, S. Welte, S. Daiss, A. Shaukat, S. Ritter, L. Li, and G. Rempe, "Deterministic creation of entangled atom–light Schrödinger-cat states," Nat. Photonics **13**, 110–115 (2019).
229. J. K. Thompson, J. Simon, H. Loh, and V. Vuletic, "A high-brightness source of narrowband, identical-photon pairs," Science **313**, 74–77 (2006).
230. J. M. Kindem, A. Ruskuc, J. G. Bartholomew, J. Rochman, Y. Q. Huan, and A. Faraon, "Control and single-shot readout of an ion embedded in a nanophotonic cavity," Nature **580**, 201–204 (2020).
231. S. Chen, M. Raha, C. M. Phenicie, S. Ourari, and J. D. Thompson, "Parallel single-shot measurement and coherent control of solid-state spins below the diffraction limit," Science **370**, 592–595 (2020).
232. A. Ruskuc, C.-J. Wu, J. Rochman, J. Choi, and A. Faraon, "Nuclear spin-wave quantum register for a solid-state qubit," Nature **602**, 408–413 (2022).
233. P.-F. Sun, Y. Yu, Z.-Y. An, J. Li, C.-W. Yang, X.-H. Bao, and J.-W. Pan, "Deterministic time-bin entanglement between a single photon and an atomic ensemble," Phys. Rev. Lett. **128**, 060502 (2022).
234. Y.-F. Pu, S. Zhang, Y.-K. Wu, N. Jiang, W. Chang, C. Li, and L.-M. Duan, "Experimental demonstration of memory-enhanced scaling for entanglement connection of quantum repeater segments," Nat. Photonics **15**, 374–378 (2021).
235. P. Wang, C.-Y. Luan, M. Qiao, M. Um, J. Zhang, Y. Wang, X. Yuan, M. Gu, J. Zhang, and K. Kim, "Experimental demonstration of memory-enhanced scaling for entanglement connection of quantum repeater segments," Nat. Commun. **12**, 233 (2021).
236. P. Drmota, D. Main, D. Nadlinger, B. Nichol, M. Weber, E. Ainley, A. Agrawal, R. Srinivas, G. Araneda, C. Ballance, and D. M. Lucas,

"Robust quantum memory in a trapped-ion quantum network node," Phys. Rev. Lett. **130**, 090803 (2023).
237. M. Balabas, T. Karaulanov, M. Ledbetter, and D. Budker, "Polarized alkali-metal vapor with minute-long transverse spin-relaxation time," Phys. Rev. Lett. **105**, 070801 (2010).
238. A. Serafin, M. Fadel, P. Treutlein, and A. Sinatra, "Nuclear spin squeezing in helium-3 by continuous quantum nondemolition measurement," Phys. Rev. Lett. **127**, 013601 (2021).
239. J. G. Bartholomew, J. Rochman, T. Xie, J. M. Kindem, A. Ruskuc, I. Craiciu, M. Lei, and A. Faraon, "On-chip coherent microwave-to-optical transduction mediated by ytterbium in YVO_4," Nat. Commun. **11**, 3266 (2020).
240. C. P. Anderson, A. Bourassa, K. C. Miao, G. Wolfowicz, P. J. Mintun, A. L. Crook, H. Abe, J. Ul Hassan, N. T. Son, T. Ohshima, and D. D. Awschalom, "Electrical and optical control of single spins integrated in scalable semiconductor devices," Science **366**, 1225–1230 (2019).
241. C. P. Anderson, E. O. Glen, C. Zeledon, A. Bourassa, Y. Jin, Y. Zhu, C. Vorwerk, A. L. Crook, H. Abe, J. Ul-Hassan, T. Ohshima, N. T. Son, G. Galli, and D. D. Awschalom, "Five-second coherence of a single spin with single-shot readout in silicon carbide," Sci. Adv. **8**, eabm5912 (2022).
242. D. B. Higginbottom, A. T. Kurkjian, and C. Chartrand, "Optical observation of single spins in silicon," Nature **607**, 266–270 (2022).
243. M. Le Dantec, M. Rančić, S. Lin, E. Billaud, V. Ranjan, D. Flanigan, S. Bertaina, T. Chanelière, P. Goldner, A. Erb, R. B. Liu, D. Estève, D. Vion, E. Flurin, and P. Bertet, "Twenty-three–millisecond electron spin coherence of erbium ions in a natural-abundance crystal," Sci. Adv. **7**, eabj9786 (2021).
244. S. Ourari, Ł. Dusanowski, S. P. Horvath, M. T. Uysal, C. M. Phenicie, P. Stevenson, M. Raha, S. Chen, R. J. Cava, N. P. de Leon, and J. D. Thompson, "Indistinguishable telecom band photons from a single erbium ion in the solid state," arXiv, arXiv:2301.03564 (2023).
245. R. Fukumori, Y. Huang, J. Yang, H. Zhang, and T. Zhong, "Subkilohertz optical homogeneous linewidth and dephasing mechanisms in Er^{3+}:Y_2O_3 ceramics," Phys. Rev. B **101**, 214202 (2020).
246. T. Rajh, L. Sun, S. Gupta, J. Yang, H. Zhang, and T. Zhong, "Hyperfine interactions and coherent spin dynamics of isotopically purified $^{167}Er^{3+}$ in polycrystalline Y_2O_3," Mater. Quantum Technol. **2**, 045002 (2022).
247. S. Gupta, X. Wu, H. Zhang, J. Yang, and T. Zhong, "Robust millisecond coherence times of erbium electron spins," Phys. Rev. Appl. **19**, 044029 (2023).
248. S. Kanai, F. J. Heremans, H. Seo, G. Wolfowicz, C. P. Anderson, S. E. Sullivan, M. Onizhuk, G. Galli, D. D. Awschalom, and H. Ohno, "Generalized scaling of spin qubit coherence in over 12,000 host materials," Proc. Natl. Acad. Sci. USA **119**, e2121808119 (2022).
249. C. M. Phenicie, P. Stevenson, S. Welinski, B. C. Rose, A. T. Asfaw, R. J. Cava, S. A. Lyon, N. P. De Leon, and J. D. Thompson, "Narrow optical line widths in erbium implanted in TiO_2," Nano Lett. **19**, 8928–8933 (2019).
250. P. Stevenson, C. M. Phenicie, I. Gray, S. P. Horvath, S. Welinski, A. M. Ferrenti, A. Ferrier, P. Goldner, S. Das, R. Ramesh, R. J. Cava, N. P. de Leon, and J. D. Thompson, "Erbium-implanted materials for quantum communication applications," Phys. Rev. B **105**, 224106 (2022).
251. Y. Wang, A. N. Craddock, R. Sekelsky, M. Flament, and M. Namazi, "Field-deployable quantum memory for quantum networking," Phys. Rev. Appl. **18**, 044058 (2022).
252. J. Kitching, "Chip-scale atomic devices," Appl. Phys. Rev. **5**, 031302 (2018).
253. J.-W. Ji, F. K. Asadi, K. Heshami, and C. Simon, "Proposal for non-cryogenic quantum repeaters with hot hybrid alkali-noble gases," arXiv, arXiv:2210.09504 (2022).
254. D. Chang, J. Douglas, A. González-Tudela, C.-L. Hung, and H. Kimble, "Colloquium: quantum matter built from nanoscopic lattices of atoms and photons," Rev. Mod. Phys. **90**, 031002 (2018).
255. Z. D. Romaszko, S. Hong, M. Siegele, R. K. Puddy, F. R. Lebrun-Gallagher, S. Weidt, and W. K. Hensinger, "Engineering of microfabricated ion traps and integration of advanced on-chip features," Nat. Rev. Phys. **2**, 285–299 (2020).
256. X. Zhou, H. Tamura, T.-H. Chang, and C.-L. Hung, "Coupling single atoms to a nanophotonic whispering-gallery-mode resonator via optical guiding," Phys. Rev. Lett. **130**, 103601 (2023).
257. P. C. Maurer, G. Kucsko, C. Latta, L. Jiang, N. Y. Yao, S. D. Bennett, F. Pastawski, D. Hunger, N. Chisholm, M. Markham, D. J. Twitchen, J. I. Cirac, and M. D. Lukin, "Room-temperature quantum bit memory exceeding one second," Science **336**, 1283–1286 (2012).
258. J.-W. Ji, Y.-F. Wu, S. C. Wein, F. K. Asadi, R. Ghobadi, and C. Simon, "Proposal for room-temperature quantum repeaters with nitrogen-vacancy centers and optomechanics," Quantum **6**, 669 (2022).
259. J. Borregaard, H. Pichler, T. Schröder, M. D. Lukin, P. Lodahl, and A. S. Sørensen, "One-way quantum repeater based on near-deterministic photon-emitter interfaces," Phys. Rev. X **10**, 021071 (2020).
260. Y. Zhan and S. Sun, "Deterministic generation of loss-tolerant photonic cluster states with a single quantum emitter," Phys. Rev. Lett. **125**, 223601 (2020).
261. P.-J. Stas, Y. Q. Huan, B. Machielse, E. N. Knall, A. Suleymanzade, B. Pingault, M. Sutula, S. W. Ding, C. M. Knaut, D. R. Assumpcao, Y.-C. Wei, M. K. Bhaskar, R. Riedinger, D. D. Sukachev, H. Park, M. Lončar, D. S. Levonian, and M. D. Lukin, "Robust multi-qubit quantum network node with integrated error detection," Science **378**, 557–560 (2022).
262. D. Awschalom, K. K. Berggren, H. Bernien, *et al.*, "Development of quantum interconnects (QuICs) for next-generation information technologies," PRX Quantum **2**, 017002 (2021).
263. M. Gündoğan, T. Jennewein, and F. K. Asadi, "Topical white paper: a case for quantum memories in space," arXiv, arXiv:2111.09595 (2021).